Heliyon 10 (2024) e36157

Contents lists available at ScienceDirect

Heliyon

journal homepage: www.cell.com/heliyon

Research article

PPAR beta/gamma mediates the antihypertensive activity of a synbiotic preparation of *Bifidobacterium lactis* and *Lactobacillus acidophilus* in spontaneous hypertensive rats

Ying Huang [a,*], Fang Wang [b], Wei Gong [c], Yufeng Chen [d]

[a] *Department of Cardiovascular, Liaoning Jin Qiu Hospital, No.317 Xiaonan Street, Shenhe District, Shenyang, Liaoning Province, 110016, China*
[b] *Department of Nursing, General Hospital of Northern Theater Command, No.83 Wenhua Road, Shenhe District, Shenyang, Liaoning Province, 110016, China*
[c] *Department of Food and Drug Inspection, Shenyang Joint Logistics Support Center Drug Instrument Supervision and Inspection Station, 53# Zhonggong Rd, Tiexi District, Shenyang, Liaoning, 110026, China*
[d] *Department of Nuclear Medicine, General Hospital of Northern Theater Command, No.83 Wenhua Road, Shenhe District, Shenyang, Liaoning Province, 110016, China*

ARTICLE INFO

Keywords:
Synbiotics
Antihypertensive activity
PPAR pathway
Proteomics
Metabolomics
Spontaneous hypertensive rat

ABSTRACT

Background: Hypertension is a global public health concern. A synbiotic preparation containing *Bifidobacterium lactis* and *Lactobacillus acidophilus* has been used as adjunct therapy for hypertension. We sought to elucidate the antihypertensive activity of this preparation and explore the underlying mechanisms.

Methods and results: Blood pressure in rats was measured using the tail-cuff method. Colonization of the gastrointestinal tract by the two probiotics was determined by real-time quantitative polymerase chain reaction (qPCR). Mechanistic studies were performed by proteomic analyses based on liquid chromatography-mass spectrometry and STRING database and metabolomic analyses using the UHPLC-Q-TOF/MS platform and peroxisome proliferator-activated receptor (PPAR)β/γ antagonists. Although biochemical analysis of blood samples showed that the synbiotic preparation did not alter the levels of angiotensin II, aldosterone, or cortisol, it significantly lowered the systolic blood pressure in the treatment group. Moreover, the synbiotic preparation contributed to the localization of the two probiotics in the ileum and colon of the treatment group. Proteomics, immunochemistry, and real-time qPCR analyses showed that administration of the synbiotic preparation activated the PPAR signaling pathway in the ileum and significantly upregulated PPARβ and PPARγ. The antagonist studies further confirmed this finding. In addition, metabolomic analyses demonstrated that among the 27 metabolites that showed significant differences between the control and model groups, administration of the synbiotic preparation significantly upregulated lysophosphatidylethanolamine and phosphatidylcholine in the ileum of the treatment group.

Conclusion: The results of the study suggest that the novel synbiotic preparation reduces blood pressure by altering the composition of the intestinal microbiota, regulating PPAR signaling pathway, and activating the PPARβ and PPARγ cascade reactions in the ileum.

* Corresponding author.
E-mail addresses: huangying0222@163.com (Y. Huang), yufengchen1978@163.com (Y. Chen).

https://doi.org/10.1016/j.heliyon.2024.e36157
Received 9 April 2024; Received in revised form 25 July 2024; Accepted 11 August 2024
Available online 13 August 2024

1. Introduction

The human gastrointestinal tract harbors approximately 1000 microbial species, which constitute approximately 90 % of all cells in the body. Human beings are considered "superorganisms" because of their close symbiotic association with the gut microbiota [1]. The interaction of the gut microbiota with ingested food, host organs, and other gut microbiota makes the gastrointestinal tract a very complex system susceptible to the effects of environmental factors, diet, medication, and age [2–5], and influences the health of the host; that is, dysbiosis of the gut microbiota can lead to the development of many diseases, such as infections, cardiovascular, and nervous system diseases. These diseases often improve when dysbiosis of the gut microbiota is corrected.

Hypertension is a global public health concern that is regarded as the most prevalent modifiable cardiovascular disease risk factor. It contributes to many complications such as stroke, kidney failure, premature death, and disability. According to epidemiological data, 1.13 billion people and >3 % of children worldwide are afflicted with hypertension [6]. The current clinical management approach for treating hypertension involves the administration of combined drugs that may induce potential adverse reactions. This often leads to poor compliance and adverse outcomes in children and older adults. Therefore, there is an urgent need to develop alternative and complementary therapies for the management of hypertension.

A synbiotic preparation containing *Lactobacillus acidophilus*, *Bifidobacterium lactis*, and xylooligosaccharides has been certified by Institute for Drug Control, the General Logistics Department of PLA (Hou Zhizi [2006] F005081) as a novel in-hospital preparation to treat hypertension. It has been used as an adjuvant strategy for the treatment of hypertension in our hospital since 2006, and has shown significant efficacy in older adults. However, reports on the antihypertensive effects of *L. acidophilus* and *B. lactis* are limited. Therefore, in this study, we aimed to further elucidate the antihypertensive activity of this synbiotic preparation and explore the underlying mechanism to provide a scientific basis for its clinical use.

2. Materials and methods

2.1. Animals

Male spontaneously hypertensive rats (SHRs) (n = 28) and Wistar Kyoto (WKY) rats (n = 14) were purchased from Beijing Vital River Laboratory Animal Technology Co., Ltd. (Beijing, China). The rats (body weight 160 ± 20 g, 6 weeks old) were housed at 21 ± 1 °C under 12-h light/12-h dark cycle (lights on at 07:00 and off at 19:00) with free access to a standard pellet diet and tap water. The rats were allowed to acclimatize to the housing facility for at least 1 week prior to the experiments. All experimental protocols were approved by the Animal Care and Use Committee of the General Hospital of Shenyang Military Area Command (No. 2016L09). Every effort was made to minimize the number of animals used and their suffering.

2.2. Experimental groups and administration of the synbiotic preparation

All rats were randomly assigned to three groups as follows: WKY control (n = 14), SHR model (n = 14), and SHR treatment (n = 14) groups. The SHR treatment group was orally administered lyophilized synbiotic preparation containing 2.5×10^9 colony forming units (CFUs) of *B. lactis*, 2.5×10^9 CFUs of *L. acidophilus,* 0.3 g of xylooligosaccharides, and maltodextrin (BioGrowing Co., Ltd., Shanghai, China) at a dose of 2.5 g/kg twice daily for 7 weeks. The WKY control and SHR model groups were treated with maltodextrin at the same dose twice daily for 7 weeks.

2.3. Blood pressure measurement

Blood pressure was measured using an automatic sphygmomanometer (Softron BP-98A; Softron, Tokyo, Japan) by the tail-cuff method [7]. To avoid blood pressure fluctuations and to obtain reliable measurements, the rats were adapted to the blood pressure monitor prior to the experiment. According to the instructions of the non-invasive blood pressure monitor system manufacturer, the animals were kept in a chamber at 38 ± 0.5 °C for 10 min, and then placed in a rodent restrainer. A cuff with an infrared sensor was

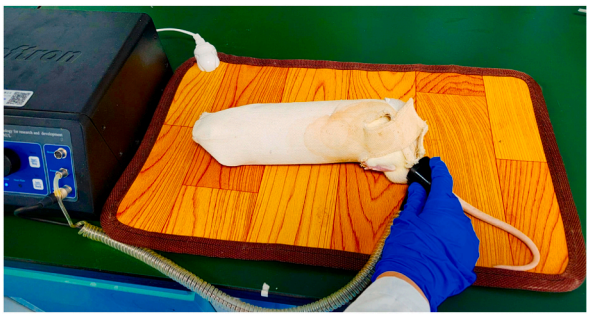

Fig. 1. Experimental photo of blood pressure measurement.

attached to the base of the tail as described previously. Systolic blood pressure (SBP) and diastolic blood pressure (DBP) were measured once the pulse stabilized. The blood pressure was measured every 3 min and averaged over three cycles. The blood pressure of each rat was measured once a week between 08:00 and 10:00 a.m. (Fig. 1).

The rats were continuously fed the synbiotic preparation for 7 weeks, following which the preparation was withheld for 2 weeks to test for withdrawal effects. The rats in the WKY control (n = 14), SHR model (n = 14), and SHR-treatment groups (n = 14) were then orally administered the synbiotic preparation or maltodextrin at the same dose twice daily for 3 weeks, starting from the 10th week. During this period, the blood pressure was measured as described above.

2.4. Blood sample analysis

Twenty-four hours after the 7th administration of the synbiotic preparation, the rats were anesthetized by intraperitoneal administration of chloral hydrate (0.3 mL/100 g) and then euthanized. Blood specimens were collected from the abdominal aorta into evacuated EDTA blood collection tubes for pretreatment from 08:00 to 10:00 a.m. Whole blood specimens (1 mL, containing 10 μL enzyme inhibitor) were centrifuged at 2200×*g* for 10 min at 4 °C to remove precipitated proteins and cell debris, and the clear supernatants were collected. The concentrations of angiotensin II (AII), aldosterone (ALD), and cortisol (COR) in the supernatants were analyzed using AII, ALD, and COR CLIA Microparticles Detection Kits (Autobio Diagnostics Co., Ltd., Zhengzhou, China), which are based on chemiluminescent magnetic microparticle immunoassay method. Briefly, 100 μL of the supernatant was mixed with 20 μL magnetic particle suspension, 50 μL antibody, and 50 μL enzyme combination and incubated for 34 min at 37 °C in a heating block according to the manufacturer's instructions. After rinsing five times with phosphate-buffered saline (PBS), the chemiluminescent substrate was added to the mixture. Chemiluminescent signals were measured using an AutoLumo A2000 analyzer (Autobio Diagnostics Co., Ltd.). Serial dilutions of the calibrators for AII (0, 10, 50, 250, 500, and 1000 ng/mL), ALD (0, 50, 100, 200, 500, and 1000 ng/mL), and COR (0, 2, 5, 10, 25, and 60 ng/mL) were used to generate the respective calibration curves. The concentrations of AII, ALD, and COR in the supernatants were calculated using the calibration curves [8].

2.5. Analysis of intestinal colonization by L. Acidophilus and B. Lactis

2.5.1. DNA extraction

Twenty-four hours after the 7th administration of the synbiotic preparation, the rats were euthanized. After collection of blood specimens, the jejunum, ileum, and colon were separated in sterile PBS (0.1 mM/L, pH 7.2), and the ingesta were gently removed. Next, the intestinal segment and mucosal surface (100 mg each) were placed in cryopreserved tubes and frozen rapidly in liquid nitrogen [9]. The samples were then stored at −80 °C.

DNA was extracted from *L. acidophilus* and *B. lactis* (from 0.1 g of synbiotic preparation), and from the jejunum, ileum, and colon specimens using the TaKaRa MiniBEST Bacteria Genomic DNA Extraction Kit (Takara Bio, Inc., Kusatsu, Japan). Briefly, the frozen samples were lysed in lysozyme solution (200 μL), treated with Rnase A, and digested with proteinase K according to the manufacturer's instructions. Finally, the DNA was eluted with 50 μL of the elution solution. All DNA samples were stored at −20 °C.

2.5.2. Polymerase chain reaction (PCR)

PCR amplification was performed in an Applied Biosystems 2720 Thermal Cycler (Applied Biosystems, Inc., Foster City, CA, USA) using *L. acidophilus* and *B. lactis* DNA extracted from the synbiotic preparation as template. The primer used for PCR are listed in Table 1, and their sequences were as described previously [10]. PCR was performed in 25-μL reaction volume containing 12.5 μL of 2 × Taq PCR MasterMix (Tiangen Biotech Co., Ltd., Beijing, China), 1 μL of forward primer (0.01 mM), 1 μL of reverse primer (0.01 mM), and 1 of μL DNA template. The reaction conditions were as follows: 94 °C for 4 min, followed by 30 cycles at 94 °C for 30 s, 56 °C for 30 s (*L. acidophilus*) or 58 °C for 30 s (*B. lactis*), and 72 °C for 1 min. An additional extension at 72 °C for 5 min was performed at the end. The amplified products (5 μL) were separated by agarose gel electrophoresis. The PCR products were purified using a DNA Fragment Purification Kit (Takara Bio Inc.).

2.5.3. DNA cloning and transformation

Purified products were cloned into the pGEM-T Easy vector (Promega, Madison, WI, USA). Ligations were performed in a 10-μL reaction mixture containing 3 μL of PCR product, 1 μL of pGEM-T Easy vector, and 1 μL of T4 DNA ligase. The reactions were incubated at 37 °C overnight. The ligation mixtures were then transformed into *Escherichia coli*. Competent cells were prepared using the heat

Table 1
Primers and probe sequences.

Target bacterial group (amplicon size)	Oligonucleotide sequence (5′–3′)
L. acidophilus (86 bp)	F: GAAAGAGCCCAAACCAAGTGATT
	R: CCCTTTCCACGGGTCCC
	5'-(FAM)-TACCACTTTGCAGTCCTACA-(BHQ-X)-3′
B. lactis (195 bp)	F: CCCTTTCCACGGGTCCC
	R: AAGGGAAACCGTGTCTCCAC
	5'-(HEX)-AAATTGACGGGGGCCCGCACAAGC-(DABCYL)-3′

shock method [11]. Briefly, the purified PCR products were added to a 50-μL aliquot of thawed competent cells. The mixture was placed on ice for 30 min, incubated in a water bath at 42 °C for 90 s for heat shock, and placed on ice for 5 min. Sterile SOC medium (500 μL) was added to the heat-shocked cells, followed by shaking at 37 °C for 1 h. Next, 100 μL of the bacterial solution was plated on LB solid medium containing 50 μg/mL ampicillin overnight at 37 °C.

2.5.4. Screening of recombinant E. coli

The colonies on the plates were tested for the presence of the target fragment using the M13 universal primer pair (F: 5′-TGTAAAACGACGGCCAGT-3′, R: 5′-CAGGAAACAGCTATGACC-3′) by PCR. PCR was performed in a 25-μL reaction mixture containing 12.5 μL of 2 × GoTaq Colorless Master Mix (Promega), 1 μL of forward primer (0.01 mM), 1 μL of reverse primer (0.01 mM), and 1 μL of bacterial template. The reaction conditions were as follows: 94 °C for 5 min, followed by 30 cycles at 94 °C for 30 s, 56 °C for 30 s, and 72 °C for 1 min. An additional extension at 72 °C for 10 min was performed at the end. The amplified products (5 μL) were separated by agarose gel electrophoresis. The cloned sequences were confirmed by sequencing [11].

2.5.5. Real-time quantitative PCR (qPCR)

Real-time qPCR assays were performed in an Applied Biosystems 7500 Fast Real-Time PCR system (Applied Biosystems) using DNA samples of the intestinal flora as template and genus-specific primer pairs (Table 1). The reaction was performed in a 20-μL mixture containing 10 μL of 2 × Premix Ex Taq (Thermo Scientific, Waltham, MA), 0.4 μL of forward primer (0.01 mM), 0.4 μL of reverse primer (0.01 mM), 0.4 of μL probe (0.01 mM), and 2 μL of DNA template. The reaction conditions were as follows: 95 °C for 30 s, followed by 40 cycles at 95 °C for 5 s, and 60 °C for 34 s. The plasmid concentrations of *L. acidophilus* and *B. lactis* were 148 ng/μL and 135 ng/μL, respectively, as measured using a Nanodrop ND 1000 spectrophotometer (Nanodrop Technologies, Wilmington, DE, USA). The copy number was calculated using the following formula: $(6.023 \times 10^{23} \times \text{plasmid amount [ng/μL]})/(\text{plasmid size [bp]} \times 10^{9} \times 650)$. Each standard curve was generated from at least six 10-fold dilutions in triplicates. Copy numbers of *L. acidophilus* and *B. lactis* in each intestinal segment were determined using the respective standard curve [12].

2.6. Metabonomic analyses

The metabolomic analysis was performed using a method described previously [13]. Briefly, 24 h after the 7th administration of the synbiotic preparation, all rats were euthanized and blood samples were collected. The ileum was separated in sterile PBS (0.1 mmol/L, pH 7.2) and the ingesta were gently removed. A section of the ileum (50 mg) was homogenized in 1 mL methanol for 2 min at 70 Hz. The mixture was centrifuged at 13,000 rpm for 15 min at 4 °C. The supernatant (200 μL) was added to the sample vial and metabonomic profiling was performed on the UHPLC-Q-TOF/MS platform. Liquid chromatography-mass spectrometry (LC-MS) analysis was performed using an Agilent 1290 Infinity LC system coupled to an Agilent 6538 Accurate-Mass Quadrupole Time-of-Flight (Q-TOF) mass spectrometer (Agilent Technologies, Santa Clara, CA, USA). Chromatographic separation was performed at 25 °C using a Waters Xselect® HSS T3 analytical column (2.1 × 100 mm, 2.5 μm; Waters, Milford, MA, USA). The mobile phases used were: (A) 0.1 % formic acid solution, and (B) I modified with 0.1 % formic acid. The flow rate was 0.4 mL/min, and the optimized gradient elution conditions were 5 % B at 0–2 min, 5–95 % B at 2–13 min, and 95 % B at 13–15 min. The MS was operated in both positive and negative ion modes. The parameters were optimized as follows: capillary voltage: 4 kV in the positive mode and 3.5 kV in the negative mode; drying gas flow: 10 L/min; gas temperature: 325 °C; nebulizer pressure: 20 psig; fragmentor voltage: 120 V; skimmer voltage: 45 V; mass range: *m/z* 100–1100; and reference ions in positive ion mode at *m/z*: 121.0509 and 922.0098, and in negative ion mode at *m/z*: 112.9856 and 1033.9881.

Raw LC-MS data were converted to common data format (.mzdata) files using the Agilent MassHunter Qualitative software. The XCMS package (http://bioconductor.org/biocLite.R) was used for peak extraction, alignment, and integration to generate a visual data matrix on the R platform. The data matrix was imported into the SIMCA-P program (version11.0; Umetrics, Umea, Sweden) for multivariate statistical analysis after weight normalization [13], including unsupervised principal component analysis and supervised partial least squares-discriminant analysis (PLS-DA). Differentially expressed metabolites were first confirmed based on their extracted molecular weights using ion flow chromatography, and their extracted molecular weights were compared with those in common online databases including the Human Metabolome Database (http://www.hmdb.ca/) and Metlin (http://metlin.scripps.edu).

2.7. Proteomics analyses

Twenty-four hours after the 7th administration of the synbiotic preparation, all rats were euthanized and whole blood samples were collected. The ileum was separated in sterile PBS (0.1 mmol/L, pH 7.2) and the ingesta were removed gently. Proteins were extracted from the ileal samples from each group, purified, and then quantified using the bicinchoninic acid assay. Then, 120 μg (20 μg/sample) of pooled proteins from each group were reduced and alkylated. Following trypsin treatment at 37 °C overnight, each pooled sample was labeled with a different tag using the iTRAQ Reagent-8Plex Multiplex Kit according to the manufacturer's instructions. The peptide mixtures were fractionated by high-pH reverse-phase LC and analyzed by LC-MS/MS (EksigentNano LC-Ultra^{TM}system tandem TripleTOFTM5600; AB SCIEX, Foster City, CA, USA) to identify differentially expressed proteins. Differentially expressed proteins were identified using ProteinPilot 4.5 software and quantified using the different tags. Under the condition of a false discovery rate of <1 %, only proteins with at least one unique peptide were considered credible, and those that changed by 1.2-fold (up or down) and showed significant ($P < 0.05$) difference were filtered as differentially expressed proteins. The STRING database contains known and predicted protein-protein interactions. The interactions include direct (physical) and indirect (functional) associations stemming from

computational predictions, knowledge transfer between organisms, and interactions taken from other primary databases. For proteomic analysis, all differentially expressed proteins were analyzed using STRING (https://string-db.org/) to identify their annotation, protein-protein interactions, and Kyoto Encyclopedia of Genes and Genomes (KEGG) pathway enrichment [14], which provided invaluable information for further exploration.

2.8. Immunofluorescence analyses

Twenty-four hours after the 7th administration of the synbiotic preparation, all rats were euthanized and whole blood samples were collected. After the ileum was separated in sterile PBS (0.1 mmol/L, pH 7.2) and the ingesta were removed gently, each ileum segment (approximately 5 mm) was embedded in OCT compound and sectioned transversely on a cryostat microtome. The sections (5 μm) were incubated overnight at room temperature in the dark with the following antibodies: anti-peroxisome proliferator-activated receptor (PPAR)α antibody (mouse anti-rat, 1:100; Thermo Fisher Scientific [MA1-822]), anti-PPARβ/δ antibody (rabbit anti-rat, 1:100; Abcam, Cambridge, MA, USA [ab23673]), and anti-PPARγ antibody (rabbit anti-rat, 1:100; Abcam [ab209350]). Subsequently, the sections were incubated for 30 min at room temperature in the dark with the corresponding secondary antibodies, including Alexa Fluor 555 (goat anti-rabbit, 1:100; Thermo Fisher Scientific [A21429]) and Alexa Fluor 488 (donkey anti-mouse, 1:100; Thermo Fisher Scientific [A21202]). Following counterstaining of the nuclei with 4′,6-diamino-2-phenylindole (DAPI; 1 mg/mL), the sections were mounted and examined using laser scanning confocal microscopy (FV1000; Olympus, Tokyo, Japan) [15]. To confirm the antibody specificity, rabbit IgG (1:100; Abcam [ab172730]) and mouse IgG2b kappa (1:100; Thermo Fisher Scientific [11-4732-42]) isotypes were used as negative controls.

2.9. Real-time qPCR analysis of PPARs

In brief, total RNA was extracted from ileal samples of the control, model, and treatment groups using an Eastep® Super RNA Extraction Kit (Promega, Beijing, China) according to the manufacturer's instructions, and stored at −80 °C. mRNA levels were analyzed using an Eppendorf BioPhotometer (Eppendorf, Hamburg, Germany). Prior to mRNA quantification, cDNA was reverse transcribed using a PrimeScript™ RT Reagent Kit (Takara Bio, Inc.) and iCycler™ 96-well Reaction Module (Bio-Rad Laboratories, Inc., Hercules, CA); reverse-transcription real-time qPCR was performed on the 7300 Fast Real-Time PCR System (Applied Biosystems) according to the manufacturer's instructions. The primer sequences used for the detection of PPARs α, β, and γ, and glyceraldehyde 3-phosphate dehydrogenase (GAPDH) are presented in Table 2. GAPDH was used as an endogenous reference gene for normalization of the expression levels of PPARs α, β, and γ. To this end, the GAPDH Ct value was subtracted from the that of the target gene, generating a ΔCt value. ΔΔCt was calculated by subtracting the mean ΔCt value of the control group from the ΔCt of the model and treatment groups. Finally, fold changes in gene expression of PPARs α, β, and γ were calculated using the comparative $2^{-\Delta\Delta Ct}$ method based on the formula: $2^{-\Delta\Delta Ct} = \Delta Ct_{\text{model/treatment}} - \Delta Ct_{\text{control}}$.

2.10. PPARβ and PPARγ antagonism tests

All rats were randomly assigned to nine groups (seven rats/group) as follows: 1) WKY control, 2) WKY control + PPARβ antagonist, 3) WKY control + PPARγ antagonist, 4) SHR model, 5) SHR model + PPARβ antagonist, 6) SHR model + PPARγ antagonist, 7) SHR treatment, 8) SHR treatment + PPARβ antagonist, and 9) SHR treatment + PPARγ antagonist groups. The SHR treatment group was orally administered a lyophilized synbiotic preparation containing 2.5×10^9 CFUs of *B. lactis*, 2.5×10^9 CFUs of *L. acidophilus,* 0.3 g of xylooligosaccharides, and maltodextrin at a dose of 2.5 g/kg twice daily for 7 weeks. The WKY control and SHR model groups were treated with maltodextrin at the same dose twice daily for 7 weeks. From the 4th week to 7th week, the WKY control, SHR model, and SHR treatment groups were administered PPARβ antagonist (GSK3787, 500 μg/kg, i.p.) and PPARγ antagonist (GW9662, 50 μg/kg, i.p.) once a day. The SBP of each rat was measured according to the protocol described in Section 2.3.

2.11. Statistical analyses

All data are presented as the mean ± standard error of the mean. The SPSS® Statistics (version 21; IBM Inc., Chicago, IL, USA) and SAS® (version 9.3; Statistical Analysis System, Inc., Raleigh, NC, USA) softwares were used for statistical analyses. The data from blood pressure measurements, blood sample analysis, analysis of the intestinal colonization by *L. acidophilus* and *B. lactis*, and real-time qPCR analysis of PPARs were subjected to analysis of variance (ANOVA) followed by Dunnett's multiple comparison test. Statistical significance was set at $P < 0.05$.

Table 2
Sequences of Primers Used for qRT-PCR.

Gene	Forward Primer	Reverse Primer
PPARα	CCCCACTTGAAGCAGATGACC	CCCTAAGTACTGGTAGTCCGC
PPARβ	AATGCCTACCTGAAAAACTTCAAC	TGCCTGCCACAGCGTCTCAAT
PPARγ	CGGAGTCCTCCCAGCTGTTCGCC	GGCTCATATCTGTCTCCGTCTTC
GAPDH	TGTGAACGGATTTGGCCGTA	GATGGTGATGGGTTTCCCGT

3. Results

3.1. Effect of the synbiotic preparation on blood pressure

The SBP and DBP of the rats in the three groups was measured once a week (Fig. 2A). Prior to treatment, both SBP and DBP of SHRs were significantly higher than those of WKY rats (152.4 ± 4.3 mmHg vs. 116.0 ± 11.5 mmHg [$P < 0.05$] and 118.3 ± 11.3 mmHg vs. 88.7 ± 9.6 mmHg [$P < 0.05$], respectively). During the seven-week treatment period, SBP was stable in the control group; however, it increased gradually in the model group and reached 183.3 ± 5.8 mmHg in the 7th week. Moreover, the synbiotic preparation significantly reduced SBP of SHRs in the treatment group from the 4th to 7th week compared with that of the model group, and reached 169.4 ± 11.4 mmHg and 168.9 ± 11.7 mmHg in the 6th and 7th weeks, respectively. However, the synbiotic preparation did not lower the DBP of SHRs, and there was no obvious difference between the DBP of SHRs in the treatment and model groups. During the treatment period, the DBP of SHRs in the model and treatment groups increased gradually and was significantly higher than that of WKY rats in the control group.

After withdrawal of the synbiotic preparation from the 7th week, the SBP of SHRs rapidly recovered in the treatment group and was almost equivalent to that in the model group in the 9th week. However, after readministration of the synbiotic preparation in the 9th week, the SBP started to decrease gradually. In the 12th week, the SBP of SHRs in the treatment group was significantly different from that in the model group. However, during this period, there was no obvious difference between the DBP of SHRs in the treatment and model groups (Fig. 2B).

3.2. Effect of the synbiotic preparation on plasma AII, ALD, and COR levels

After seven weeks of treatment with the synbiotic preparation, the plasma levels of AII, ALD, and COR of SHRs in the model group

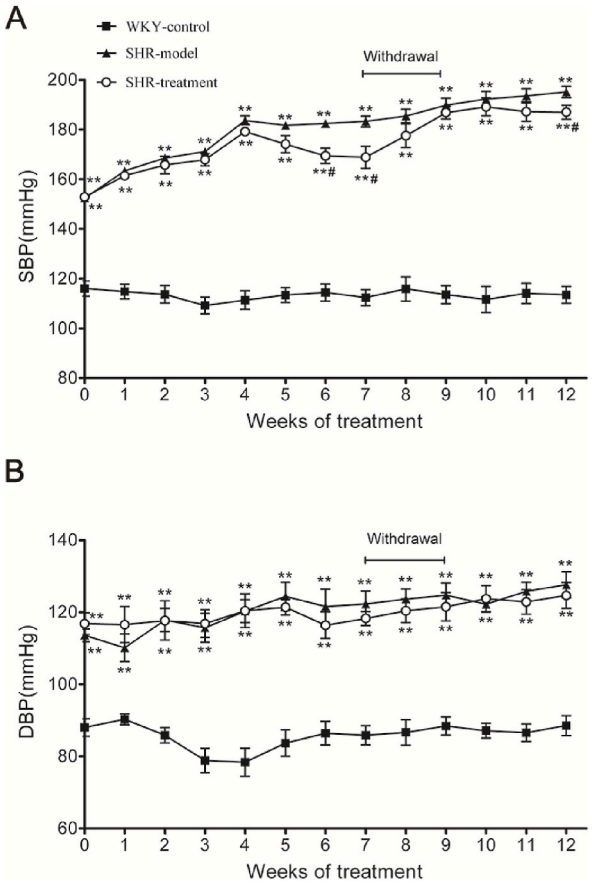

Fig. 2. Effects of synbiotics on systolic blood pressure (A) and diastolic blood pressure (B). After SHR rats and WKY rats were administered synbiotics or maltodextrin continuously for 7 weeks, the withdrawal test was performed for 2 weeks, followed by readministered synbiotics or maltodextrin for three weeks from 10th week. The dots were presented as the mean ± standard error of the mean. Asterisks indicated statistical significance between the SHR-model or the SHR-treatment group and the WKY-control group on the same week, $^{**}p < 0.01$. Symbol indicated statistical significance between the SHR-model and the SHR-treatment groups on the same week, $\#p < 0.05$.

were significantly higher than those of WKY rats in the control group (Table 3), indicating that the renin-angiotensin-aldosterone system (RAAS) may be involved in the pathogenesis of spontaneous hypertension in SHRs. However, there was no significant difference in the plasma concentration of AII, ALD, and COR between the model and treatment groups, indicating that the antihypertensive mechanism of the synbiotic preparation was not related to the RAAS.

3.3. Effect of the synbiotic preparation on the intestinal colonization by L. Acidophilus and B. Lactis

To study the colonization of the intestinal segments by *L. acidophilus* and *B. lactis*, real-time qPCR assays were performed and standard curves were generated by regression analysis. The standard curves of *L. acidophilus* and *B. lactis* were $y = -3.338x + 41.65$ and $y = -3.171x + 43.41$ (Fig. 3A and B); the coefficient correlations were 0.9997 and 0.9991, and the efficiencies were 99.3 % and 106.7 %, respectively.

Following 7 weeks of continuous administration of the synbiotic preparation, *L. acidophilus* and *B. lactis* predominantly colonized the ileum and colon; however, not the jejunum in the treatment group. In addition, the number of *L. acidophilus* that colonized the ileum and colon of SHRs in the treatment group were significantly higher than those of SHRs in the model group and WKY rats in the control group. The number of *B. lactis* that colonized the ileum of SHRs in the treatment group were significantly higher than those in the model group and WKY rats in the control group. However, the number of *B. lactis* in the colon of SHRs in the treatment group was almost equal to that in the control group and significantly higher than that in the model group. Moreover, the number of *L. acidophilus* colonizing the ileum in the model group was lower than that in the control group. These results indicated that the synbiotic preparation contributed to the colonization of the ileum and colon of SHRs by *L. acidophilus* and *B. lactis* and thus altered the composition of their gut microbiota (Fig. 3C and D).

3.4. Metabonomic analysis of the antihypertensive effect of the synbiotic preparation in the ileum

Gut microbiota produce thousands of metabolites through interactions with the host and partially digested food. These microbial metabolites are absorbed from the gut and play specific roles in pathological and physiological processes involved in an individual's susceptibility to disease and/or treatment outcomes. In the last decade, metabolomics has emerged as a systems biology approach to obtain valuable insights into intra- and extracellular regulatory processes involved in host-gut microbial metabolic interactions because of its ability to monitor metabolic variations and detect the adaptive multiparametric responses of an organism to exogenous stimuli in real time using MS. The PLS-DA model, a supervised multivariate statistical analysis method, was applied to visualize the trends in the control, model, and treatment groups. As illustrated by the PLS-DA score plots of the three groups in both the electrospray ionization-positive and -negative modes (Fig. 4A and B), the control group was clearly separated from the model and treatment groups in the first principal component. The samples in the treatment group were located between the control and model groups in the first principal component, indicating that the metabolic profile of the model group was clearly altered compared with that of the control group and that the synbiotic preparation had a definite therapeutic effect on the model group. Supervised PLS-DA was applied to identify the differentially regulated metabolites between the model and control groups. Score plots from the PLS-DA model (Fig. 4C and D) showed that the model group was clearly separated from the control group, indicating significant differences between the metabolic profiles of the model and control groups. When the two components were calculated, the cumulative R2X, R2Y, and Q2 values were 0.419, 0.937, and 0.693, respectively, in the positive mode, and 0.565, 0.942, and 0.826, respectively, in the negative mode. These values showed that the PLS-DA model had a good degree of fit and predictive ability to screen differential variables between the groups. Scatter plots of the PLS-DA model (Fig. 4E and F) illustrate the contribution of different metabolite ions to the differences between the groups. Each dot on the plot represents an ion of a metabolite. The farther the dot from the origin point, the more significant its contribution to the differences between the groups, as indicated by larger corresponding variable importance (VIP) values. The VIP value, which was generated in the PLS-DA processing, represents the contribution of the ions in discriminating between the groups [13]. Ions with VIP values > 1.0 were considered candidate differential ions. ANOVA and Tukey's *post-hoc* tests were performed to assess the significance of the differences among the three groups. Finally, as determined by P (M/C) values ($P < 0.05$), 27 metabolites that were significantly different between the control and model groups were identified (Table 4). Moreover, the P (T/M) values ($P < 0.05$) revealed that among the 27 metabolites, lysophosphatidylethanolamine (lysoPE) and phosphatidylcholines (PCs) were significantly upregulated in the treatment group compared with that in the model group following administration of the synbiotic

Table 3
Effects of synbiotics on the levels of plasma AII, ALD and COR after administered continuously for 7 Weeks.

Index	WKY-control (n = 7)	SHR-model (n = 7)	SHR-treatment (n = 7)
AII (pg/ml)	187.2 ± 37.43	234.1 ± 36.14*	230.7 ± 36.04*
ALD (pg/ml)	278.9 ± 42.49	324.9 ± 52.57*	313.8 ± 35.72*
COR (μg/dl)	6.291 ± 1.965	7.246 ± 1.043*	6.991 ± 0.986*

Table 3 After administered synbiotics for 7 weeks, the concentrations of AII, ALD and COR in the plasma of SHRs in the both model and treatment groups exhibited significant higher than those of WKYs in the control group. However, there were not significant differences in the concentrations of AII, ALD and COR in the plasma between the model and treatment groups. Results were expressed as the mean ± standard error of the mean. Asterisks indicated statistical significance between the SHR-model or the SHR-treatment group and the WKY-control group,*$p < 0.05$. AII: AngiotensinII; ALD: aldosterone; COR: cortisol.

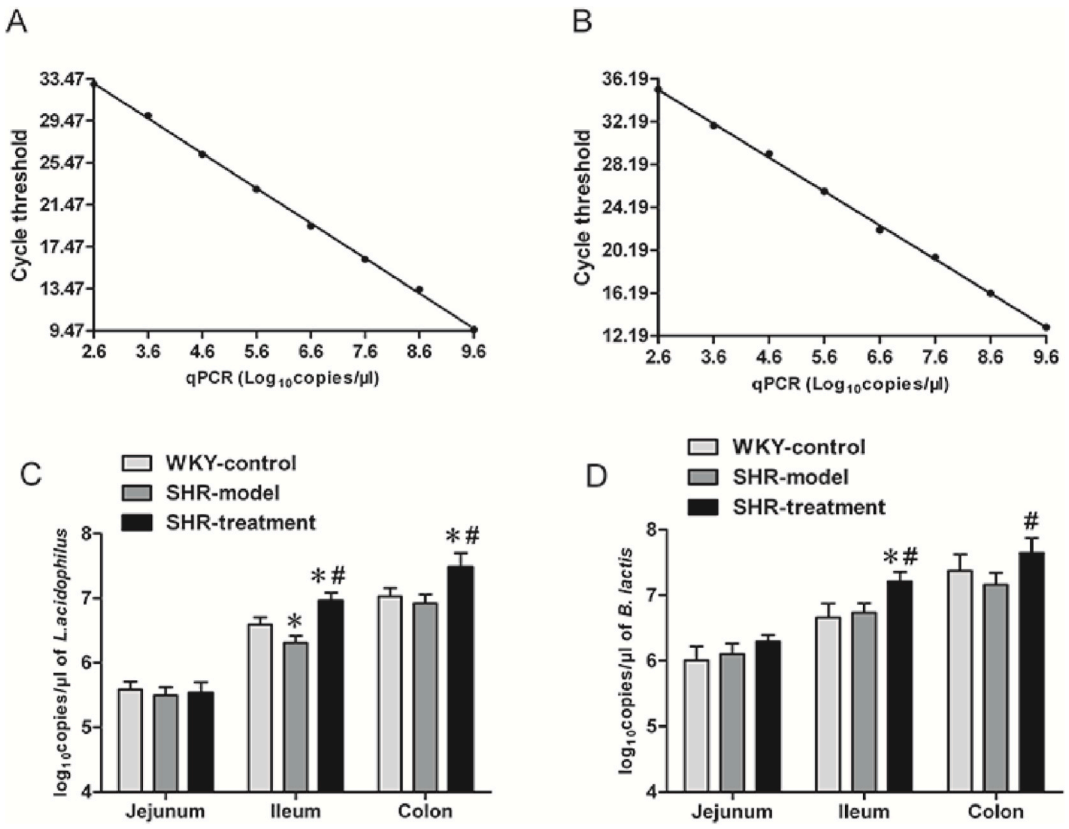

Fig. 3. (A) & (B): Standard curves of *L. acidophilus* and *B. lactis*, which were established from at least six 10-fold dilutions of plasmids measured by real-time qPCR assay. The standard curves of *L. acidophilus* and *B. lactis* were y = −3.338x + 41.65 and y = −3.171x + 43.41, respectively. The coefficient correlations were 0.9997 and 0.9991 and the efficiencies were 99.3 % and 106.7 %, respectively. (C) & (D): The quantities of *L. acidophilus* and *B. lactis* colonized in the jejunum (n = 7), ileum (n = 7) and colon (n = 7) after continuous administration of synbiotics for 7 weeks. Results were expressed as the mean ± standard error of the mean. Asterisks indicated statistical significance between the SHR-model or the SHR-treatment group and the WKY-control group, $^{*}p < 0.05$. Symbol indicated statistical significance between the SHR-model and the SHR-treatment groups, #p < 0.05.

preparation.

3.5. Proteomic analysis of the antihypertensive effect of the synbiotic preparation in the ileum

STRING analysis revealed the interaction network between the differentially expressed proteins and enriched the pathways according to the KEGG database. In this study, 71 proteins were differentially expressed in the ileum between the model and control groups (P (M/C) < 0.05), among which 38 were upregulated (fold change (M/C) > 1.20) and 33 were downregulated (fold change (M/C) < 0.80) (Table 5). Pathway enrichment analysis of these 71 differentially expressed proteins revealed that the PPAR signaling pathway exhibited the highest score (Fig. 5), with six of the differentially expressed proteins were related to this pathway (Table 6). In addition, STRING network analysis of the differentially expressed proteins confirmed the interactions among the proteins related to the PPAR signaling pathway (Fig. 6).

Following administration of the synbiotic preparation, 26 out of the 71 differentially expressed proteins were reregulated ([fold change (T/M) < 0.80, fold change (M/C) > 1.20] or [fold change (T/M) > 1.20 and fold change (M/C) < 0.80]) in the ileum of SHRs (Table 5). Notably, among the six differentially expressed proteins involved in the PPAR signaling pathway, retinoic acid receptor beta (RXRβ), a key protein, was significantly reregulated (P (T/M) < 0.05) following administration of the synbiotic preparation (Table 5).

3.6. Immunofluorescence analysis

To confirm the results of the proteomics analysis and to identify the PPAR subtype that plays an important role in the antihypertensive mechanism, the expression of PPARs α, β, and γ was determined by immunohistochemistry. The data showed that following 7 weeks of continuous administration of the synbiotic preparation, the expression of PPARα in the ileum was significantly downregulated in the SHR model and SHR treatment groups compared with that in the WKY group (Fig. 7A), which indicated that the synbiotic preparation had no effect on PPARα expression in SHRs. However, the expression of PPARβ and γ in the ileum was

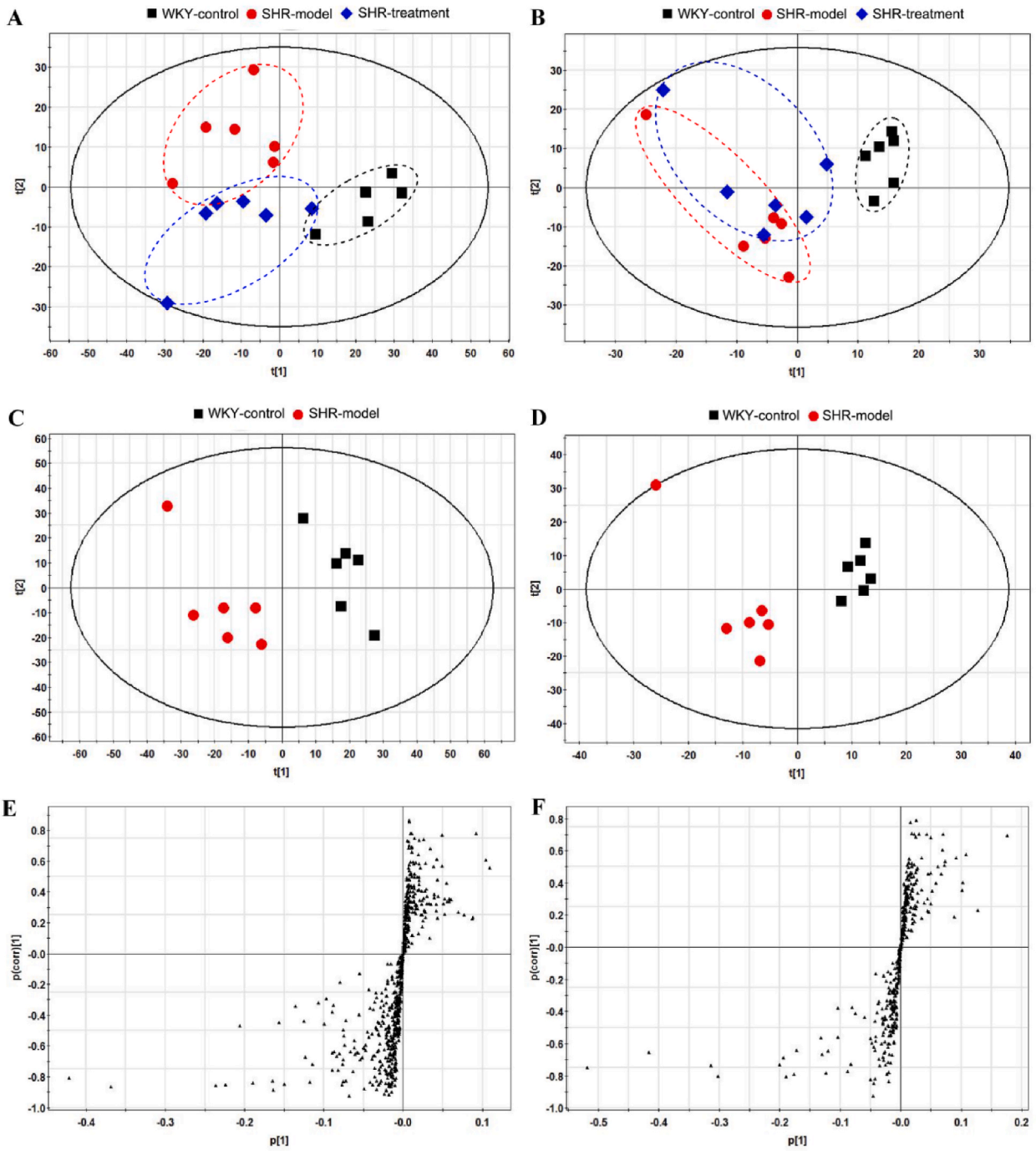

Fig. 4. Plots of multivariate statistical analysis based on variables of the control, model and treatment group. (A) PLS-DA scores plot of three groups in ESI positive mode; (B) PLS-DA scores plot of three groups in ESI negative mode; (C) PLS-DA scores plot of the control and model group in ESI positive mode; (D) PLS-DA scores plot of the control and model group in ESI negative mode; Each dot or diamond in the figure represents one sample in each group. (E) PLS-DA Scatter plot of the control and model group in ESI positive mode; (F) PLS-DA Scatter plot of the control and model group in ESI negative mode. Each dot represents an ion of metabolite.

significantly upregulated in the SHR treatment group compared with that in the SHR model group, and their levels were almost the same as that in the WKY group (Fig. 7B and C). These data indicated that the synbiotic preparation upregulates the expression of PPARβ and γ in the ileum of the SHR treatment group to attenuate blood pressure.

Table 4
The different metabolites in the control, model and treatment groups.

No.	*m/z*	Rt (min)	VIP	FC(M/C)	p (M/C)	FC(T/M)	p (T/M)	Ion	Formula	Metabolites	Related pathway
1	259.023	0.73	1.74	1.50	0.0051	0.97	0.9328	[M − H]-	C6H13O9P	D-Glucose 6-phosphate	Inositol phosphate metabolism
2	167.02	0.88	2.41	0.79	0.0295	1.16	0.2239	[M − H]-	C5H4N4O3	Uric acid	Purine metabolism
	169.035	1.00	1.40	0.74	0.0120	1.05	0.8666	[M+H]+	C5H4N4O3	Uric acid	Purine metabolism
3	133.032	1.00	1.49	1.27	0.0439	1.04	0.8597	[M+H]+	C5H8O2S	THTC	–
4	346.055	1.02	1.02	2.35	0.0015	1.15	0.5178	[M − H]-	C10H14N5O7P	Adenosine monophosphate	cAMP signaling pathway
5	153.04	1.03	2.01	3.90	0.0318	0.53	0.2117	[M+H]+	C5H4N4O2	Xanthine	Purine metabolism
6	318.3	9.31	1.17	1.95	0.0491	0.56	0.0763	[M+H]+	C18H39NO3	Phytosphingosine	Sphingolipid metabolism
7	526.294	10.16	1.03	1.41	0.0022	0.89	0.2746	[M+H]+	C27H44NO7P	LysoPE (22:6/0:0)	Glycerophospholipid metabolism
8	502.293	10.17	1.79	1.39	0.0013	0.81	0.0228	[M+H]+	C25H44NO7P	LysoPE (20:4/0:0)	Glycerophospholipid metabolism
9	506.36	10.55	1.07	1.44	0.0419	0.98	0.9866	[M+H]+	C26H52NO6P	C-8 Ceramide-1-phosphate	Sphingolipid metabolism
10	526.351	10.87	3.93	0.46	0.0014	1.00	1.0000	[M + FA-H]-	C24H52NO6P	Lyso-PAF C-16	Glycerophospholipid metabolism
11	917.628	10.89	1.72	0.42	0.0009	1.30	0.5811	[M − H]-	C49H91O13P	PI(18:0/22:2)	Glycerophospholipid metabolism
12	873.574	10.93	2.10	0.66	0.0313	1.05	0.9599	[M − H]-	C50H83O10P	PG (22:6)/22:2)	Glycerophospholipid metabolism
13	524.336	10.96	3.24	1.98	0.0121	1.17	0.5210	[M + FA-H]-	C24H50NO6P	LysoPC(P-16:0)	Glycerophospholipid metabolism
14	450.299	11.55	1.33	0.82	0.0366	1.06	0.7314	[M − H]-	C22H46NO6P	PC(O-14:1/0:0)	Glycerophospholipid metabolism
15	494.36	12.40	1.10	2.05	0.0277	0.85	0.6780	[M+H]+	C25H52NO6P	PE (P-20:0/0:0)	Glycerophospholipid metabolism
16	536.407	12.49	2.18	1.55	0.0032	0.88	0.3748	[M+H]+	C28H58NO6P	PC(P-20:0/0:0)	Glycerophospholipid metabolism
17	280.263	12.68	1.19	1.61	0.0267	0.71	0.1011	[M+H]+	C18H33NO	Linoleamide	–
18	327.233	13.22	3.81	1.28	0.0041	0.93	0.4296	[M − H]-	C22H32O2	Docosahexaenoic acid	Biosynthesis of unsaturated fatty acids
19	835.664	13.39	1.92	2.47	0.0130	0.86	0.7194	[M+Na]+	C47H93N2O6P	SM(d18:2/24:0)	Sphingolipid metabolism
20	833.631	13.39	2.93	0.29	0.0004	1.28	0.8284	[M+H]+	C46H89O10P	PG (18:0/22:1)	Glycerophospholipid metabolism
21	303.232	13.40	6.54	1.20	0.0111	0.97	0.8438	[M − H]-	C20H32O2	Arachidonic Acid	Arachidonic acid metabolism
22	804.552	13.57	5.58	2.09	0.0038	0.61	0.0265	[M+Na]+	C44H80NO8P	PC(16:0/20:4)	Glycerophospholipid metabolism
23	494.361	13.75	1.35	1.36	0.0335	0.92	0.6982	[M − H]-	C25H54NO6P	PE (O-20:0/0:0)	Glycerophospholipid metabolism
24	305.248	13.82	1.42	1.39	0.0081	0.84	0.1581	[M − H]-	C20H34O2	Eicosatrienoic Acid	Linoleic acid metabolism
25	538.423	13.94	3.21	1.53	0.0267	0.88	0.5969	[M+H]+	C28H60NO6P	PC(O-20:0/0:0)	Glycerophospholipid metabolism
26	331.264	14.09	3.92	1.32	0.0171	0.96	0.8416	[M − H]-	C22H36O2	Docosatetraenoic Acid	Biosynthesis of unsaturated fatty acids
27	281.248	14.26	3.10	1.31	0.0027	0.93	0.4364	[M − H]-	C18H34O2	Oleic Acid	Fatty acid biosynthesis

Table 4 Determined by P (M/C) values ($P < 0.05$), 27 metabolites with significant differences between the control and model group were identified by the method of metabonomics analysis. Moreover, among 27 metabolites, lysophosphatidylethanolamine (LysoPE) and phosphatidylcholines (PC) could be significantly reregulated in the treatment group after the administration of synbiotics, compared with the model group, which was determined by P (T/M) values ($P < 0.05$). m/z: mass charge ratio; Rt: rational time; VIP: variable importance; FC: fold change; M/C: model/control; T/M: treatment/model.

Table 5
The differentially expressed proteins in the control, model and treatment groups.

No.	Accession	Name	Gene	Peptides (95 %)	Fold Change (M/C)	P (M/C)	Fold Change (T/M)	P (T/M)
1	Q62812	Myosin-9	MYH9	192	0.7311	0.0001	1.1272	0.2136
2	D3ZHA0	Filamin-C	FLNC	103	0.5495	0.0001	1.7701	0.0202
3	P07335	Creatine kinase B-type	KCRB	92	0.5546	0.0022	0.6982	0.8360
4	P48037	Annexin A6	ANXA6	48	0.5200	0.0013	1.6293	0.0081
5	Q63270	Cytoplasmic aconitate hydratase	ACOC	32	0.6668	0.0478	1.3552	0.3422
6	P22985	Xanthine dehydrogenase/oxidase	XDH	31	0.7447	0.0479	1.1376	0.2121
7	Q62635	Mucin-2 (Fragment)	MUC2	29	0.3802	0.0007	1.0000	0.8674
8	Q5RKI0	WD repeat-containing protein 1	WDR1	34	0.7447	0.0361	1.3677	0.0731
9	Q9Z1X1	Extended synaptotagmin-1	ESYT1	17	0.6607	0.0285	1.4060	0.1628
10	P98089	Intestinal mucin-like protein (Fragment)	MUC2L	21	0.3767	0.0092	1.2942	0.8671
11	Q08163	Adenylyl cyclase-associated protein 1	CAP1	27	0.6427	0.0155	0.9036	0.9856
12	Q62952	Dihydropyrimidinase-related protein 3	DPYL3	23	0.6607	0.0356	0.6427	0.6558
13	F1LQ48	Heterogeneous nuclear ribonucleoprotein L	HNRPL	25	0.5649	0.0152	0.8710	0.6664
14	Q5XI07	Lipoma-preferred partner homolog	LPP	17	0.4325	0.0420	1.1272	0.8142
15	Q497B0	Omega-amidase NIT2	NIT2	11	0.4831	0.0090	0.8241	0.7662
16	Q9Z1Z9	PDZ and LIM domain protein 7	PDLI7	15	0.6081	0.0461	0.9727	0.5253
17	P07150	Annexin A1 OS=Rattus norvegicus	ANXA1	15	0.3281	0.0189	2.9923	0.0057
18	P14046	Alpha-1-inhibitor 3	A1I3	38	0.4699	0.0453	1.7701	0.0171
19	P54290	Voltage-dependent calcium channel subunit α-2/Δ-1	CA2D1	9	0.3192	0.0019	2.4889	0.0766
20	Q6IFW6	Keratin, type I cytoskeletal 10	K1C10	13	0.3733	0.0090	2.3988	0.0732
21	Q10728	Protein phosphatase 1 regulatory subunit 12A	MYPT1	13	0.5546	0.0203	1.2246	0.5933
22	O35413	Sorbin and SH3 domain-containing protein 2	SRBS2	8	0.4786	0.0462	0.9120	0.4625
23	Q9WUH4	Four and a half LIM domains protein 1	FHL1	11	0.5649	0.0127	1.2474	0.6657
24	Q66H12	Alpha-N-acetylgalactosaminidase	NAGAB	9	0.7379	0.0419	0.7870	0.8217
25	P42123	L-lactate dehydrogenase B chain	LDHB	9	0.4207	0.0263	1.4191	0.2011
26	P18163	Long-chain-fatty-acid–CoA ligase 1	ACSL1	10	0.5970	0.0188	0.9817	0.8839
27	P14141	Carbonic anhydrase 3	CAH3	6	0.5248	0.0420	1.3932	0.4506
28	Q07969	Platelet glycoprotein 4	CD36	6	0.2992	0.0094	0.8241	0.6546
29	Q02765	Cathepsin S	CATS	8	0.4831	0.0369	1.6293	0.1728
30	P58775	Tropomyosin beta chain	TPM2	29	0.4613	0.0447	0.6252	0.4235
31	O08837	Cell division cycle 5-like protein	CDC5L	3	0.6855	0.0481	1.1482	0.2812
32	Q63010	Liver carboxylesterase B-1	EST5	4	0.4966	0.0047	2.5119	0.0050
33	P16086	Spectrin alpha chain, non-erythrocytic 1	SPTN1	100	1.2942	0.0282	1.1695	0.2841
34	P02770	Serum albumin	ALBU	138	1.8880	0.0269	1.3804	0.0000
35	P07756	Carbamoyl-phosphate synthase, mitochondrial	CPSM	46	1.4859	0.0035	0.8551	0.4272
36	P01026	Complement C3	CO3_	43	1.3428	0.0373	1.1066	0.1617
37	P06685	Sodium/potassium-transporting ATPase subunit α-1	AT1A1	80	1.6904	0.0196	0.8472	0.3237
38	P55281	Cadherin-17	CAD17	27	2.0893	0.0082	0.9120	0.0814
39	Q63041	Alpha-1-macroglobulin	A1M	29	2.0137	0.0147	1.3804	0.0660
40	P28037	Cytosolic 10-formyltetrahydrofolate dehydrogenase	AL1L1	24	1.8707	0.0006	1.0471	0.9649
41	P15684	Aminopeptidase N	AMPN	41	1.9588	0.0051	1.0765	0.2186
42	P55260	Annexin A4	ANXA4	37	1.4588	0.0339	0.7870	0.9124
43	P50123	Glutamyl aminopeptidase	AMPE	23	1.5276	0.0198	0.9817	0.2151
44	P82808	Glutamine–fructose-6-phosphate aminotransferase 1	GFPT1	30	1.7865	0.0153	0.5200	0.0525
45	O54728	Phospholipase B1, membrane-associated	PLB1	16	2.1677	0.0206	1.1272	0.9222
46	P07872	Peroxisomal acyl-coenzyme A oxidase 1	ACOX1	21	1.9231	0.0014	1.0280	0.5170
47	Q5SGE0	Leucine-rich PPR motif-containing protein	LPPRC	16	1.8707	0.0067	0.7516	0.1874
48	Q68FS4	Cytosol aminopeptidase	AMPL	20	1.4997	0.0356	0.8790	0.2671
49	Q6Q0N1	Cytosolic non-specific dipeptidase	CNDP2	24	1.2942	0.0067	1.0765	0.7875
50	Q5XHZ0	Heat shock protein 75 kDa, mitochondrial	TRAP1	18	1.6596	0.0305	0.7447	0.1331
51	P25409	Alanine aminotransferase 1	ALAT1	17	1.4191	0.0291	0.8710	0.2152
52	O54697	N-acetylated-α-linked acidic dipeptidase-like protein	NALDL	24	1.6904	0.0103	0.8551	0.6989
53	Q9QZA2	Programmed cell death 6-interacting protein	PDC6I	15	1.4859	0.0488	0.8790	0.5099
54	Q62774	Unconventional myosin-Ia	MYO1A	25	1.2359	0.0166	1.0666	0.9077
55	P18886	Carnitine O-palmitoyltransferase 2, mitochondrial	CPT2	12	1.6444	0.0420	0.9908	0.4667
56	P28826	Meprin A subunit beta	MEP1B	12	1.7701	0.0048	1.2474	0.7813
57	P51538	Cytochrome P450 3A9	CP3A9	11	5.7016	0.0190	0.9036	0.4332
58	P06399	Fibrinogen alpha chain	FIBA	11	1.9588	0.0498	0.9908	0.6370
59	P43245	Multidrug resistance protein 1	MDR1	13	2.2699	0.0008	1.0093	0.2770
60	P04639	Apolipoprotein A-I	APOA1	14	2.2080	0.0244	0.7943	0.4474

(*continued on next page*)

Table 5 (*continued*)

No.	Accession	Name	Gene	Peptides (95 %)	Fold Change (M/C)	P (M/C)	Fold Change (T/M)	P (T/M)
61	Q63269	Inositol 1,4,5-trisphosphate receptor type 3	ITPR3	7	1.9953	0.0090	0.5916	0.4216
62	P51574	Solute carrier family 15 member 1	S15A1	6	2.7542	0.0213	1.3062	0.7479
63	P51870	Cytochrome P450 4F5	CP4F5	7	3.6644	0.0138	1.0186	0.9775
64	P16446	Phosphatidylinositol transfer protein alpha isoform	PIPNA	5	1.6749	0.0206	1.0765	0.2475
65	P62994	Growth factor receptor-bound protein 2	GRB2	5	2.8840	0.0407	1.0666	0.8967
66	P05982	NAD(P)H dehydrogenase [quinone] 1	NQO1	7	6.3680	0.0105	0.6855	0.4866
67	P02651	Apolipoprotein A-IV	APOA4	4	2.2699	0.0157	0.3802	0.0317
68	P01836	Ig kappa chain C region, A allele	KACA	5	3.6644	0.0272	0.9638	0.7284
69	P43244	Matrin-3	MATR3	4	2.9648	0.0352	0.5152	0.5355
70	Q6TA48	Mucosal pentraxin	MPTX	4	3.6308	0.0247	1.3932	0.5832
71	P49743	Retinoic acid receptor RXR-beta	RXRB	2	0.6026	0.0414	1.5417	0.0454

Table 5 71 differentially expressed proteins in the ileum between the model and control group ($P(M/C) < 0.05$) were determined by the method of proteomics analysis, among which 38 were upregulated (Fold Change(M/C) > 1.20) and 33 were downregulated (Fold Change(M/C) < 0.80). After administration of synbiotics, 26 of 71 proteins were reregulated in the ileum of the treatment group [(Fold Change(T/M) < 0.80 and Fold Change(M/C) > 1.20) or (Fold Change(T/M) > 1.20 and Fold Change(M/C) < 0.80)]. M/C: model/control; T/M: treatment/model.

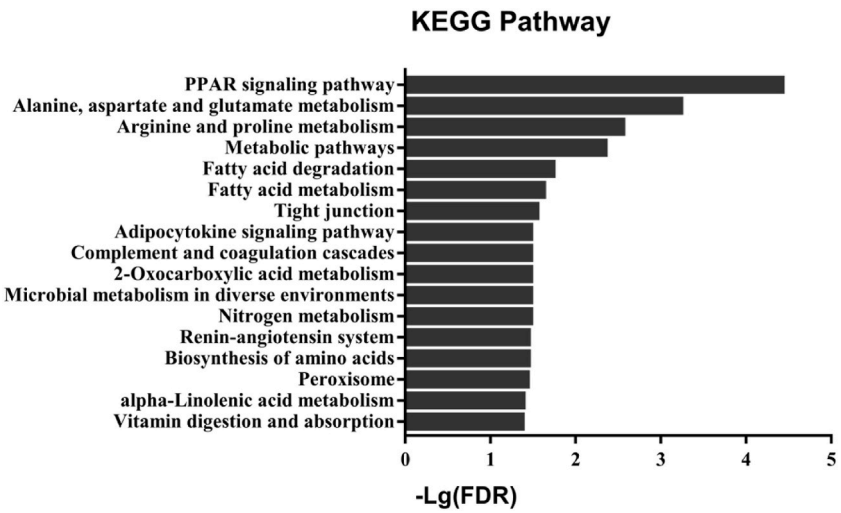

Fig. 5. Kegg pathway enrichment analysis.

Table 6
The differentially expressed proteins related to PPAR signaling pathway.

Uniport Accession	Name	Molecular function
Q07969	CD36 molecule (Cd36)	lipoprotein particle binding, lipid binding, fatty acid binding
P07872	acyl-CoA oxidase 1(Acox1)	fatty-acyl-CoA binding, acyl-CoA oxidase activity, fatty acid binding
P18163	acyl-CoA synthetase long-chain family member 1 (Acsl1)	acetate-CoA ligase activity, long-chain fatty acid-CoA ligase activity
P04639	apolipoprotein A1 (Apoa1)	lipid transporter activity, phospholipid binding, lipid binding
P18886	carnitine palmitoyltransferase 2(Cpt2)	Carnitine O-palmitoyltransferase activity
P49743	Retinoic acid receptor RXR-beta	ligand-activated sequence-specific DNA binding, steroid hormone receptor activity

Table 6 Compared with the WKYs, six differentially expressed proteins involved in PPAR signaling pathway were determined in the ileum segment of SHRs by the method of proteomics analysis.

3.7. Real-time qPCR analysis of PPARs

Real-time qPCR demonstrated that PPARα expression was significantly downregulated in the model and treatment groups compared with that in the control group. Moreover, expression of PPARβ and γ was significantly downregulated in the model group compared with that in the control group; however, the expression of PPARβ and γ was markedly upregulated in the treatment group

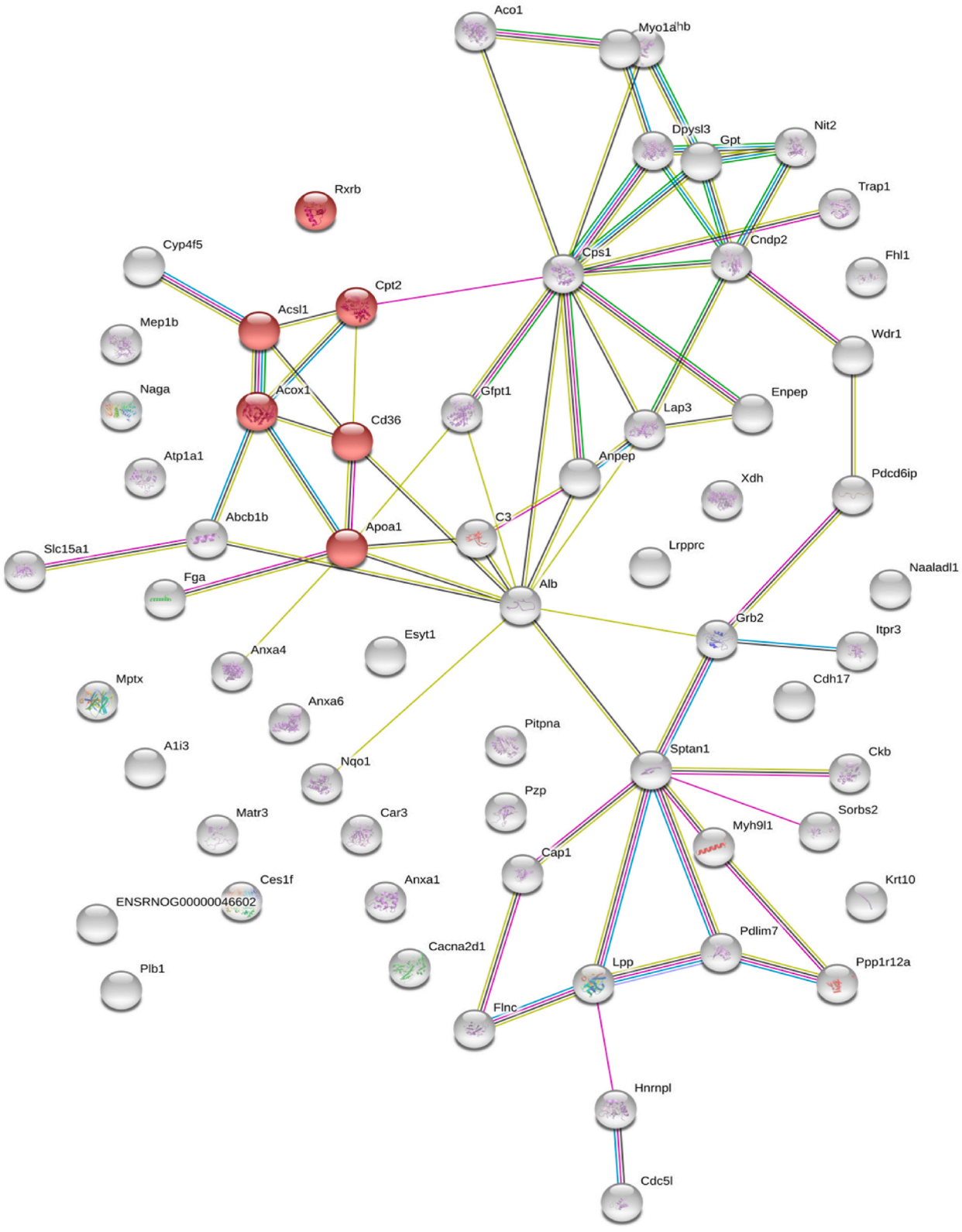

Fig. 6. Network Analysis of differentially expressed proteins. Among these proteins, the six red balls represented the proteins related to PPAR signaling pathway (Rxrb, Acsl1, Cpt2, Acox1, CD36 and Apoa1). The lines between balls represented as follows.

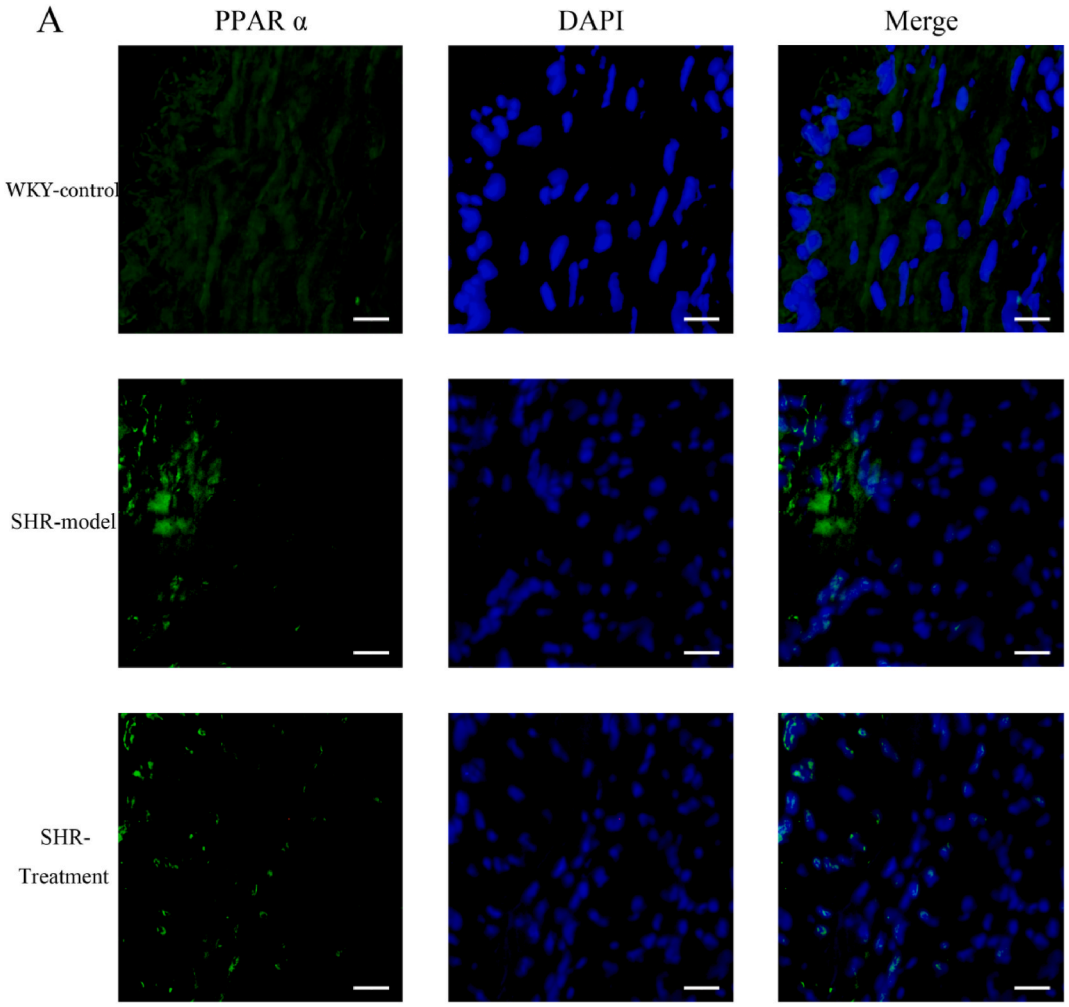

Fig. 7. (Ã C) The expressions of PPARα, β and γ in the ileum segment of WKY, SHR-model and SHR-treatment groups. In the left column, the sections of ileum in WKY, SHR-model and SHR-treatment groups were stained with PPARα, β and γ antibody. PPARα exhibited green and PPARβ and γ exhibited red. In the middle column, the sections of ileum in WKY, SHR-model and SHR-treatment groups were counterstained with DAPI, and the nuclei in the ileum segment became blue. In the right column, here were merge images of PPARα, β and γ and DAPI in the ileum of WKY, SHR-model and SHR-treatment groups. (D) The negative control of PPARα, β and γ. Bar: 20 μm.

compared with that in the model group after the administration of the synbiotic preparation. In addition, the expression of PPARβ; however, not PPARγ, was markedly downregulated after the administration of the synbiotic preparation, compared with that in the control group (Fig. 8).

3.8. Effects of PPARβ and PPARγ antagonists

In the first 4 weeks, the SBP showed no significant difference between the SHR model and SHR-treatment groups; however, there were marked differences between the SHR and WKY control groups. However, from week 4 to week 7, the SBP of the SHR-treatment group was lower than that of the SHR model group.

When the rats were administered the PPARβ (GSK3787) or PPARγ (GW9662) antagonists, the antihypertensive effect of synbiotic preparation in the SHR treatment group was significantly inhibited from week 4 to week 7. The SBP of the SHR-treatment group administered the antagonist showed no difference compared to that of the SHR model group with or without antagonists; however, the SBP was significantly different compared to that of the SHR-treatment group without antagonist. The SBP in the two SHR model groups showed no significant difference with or without the antagonist. Furthermore, the SBP was not significantly different between WKY control and WKY control + PPARβ antagonist or PPARγ antagonist groups (Fig. 9A and B).

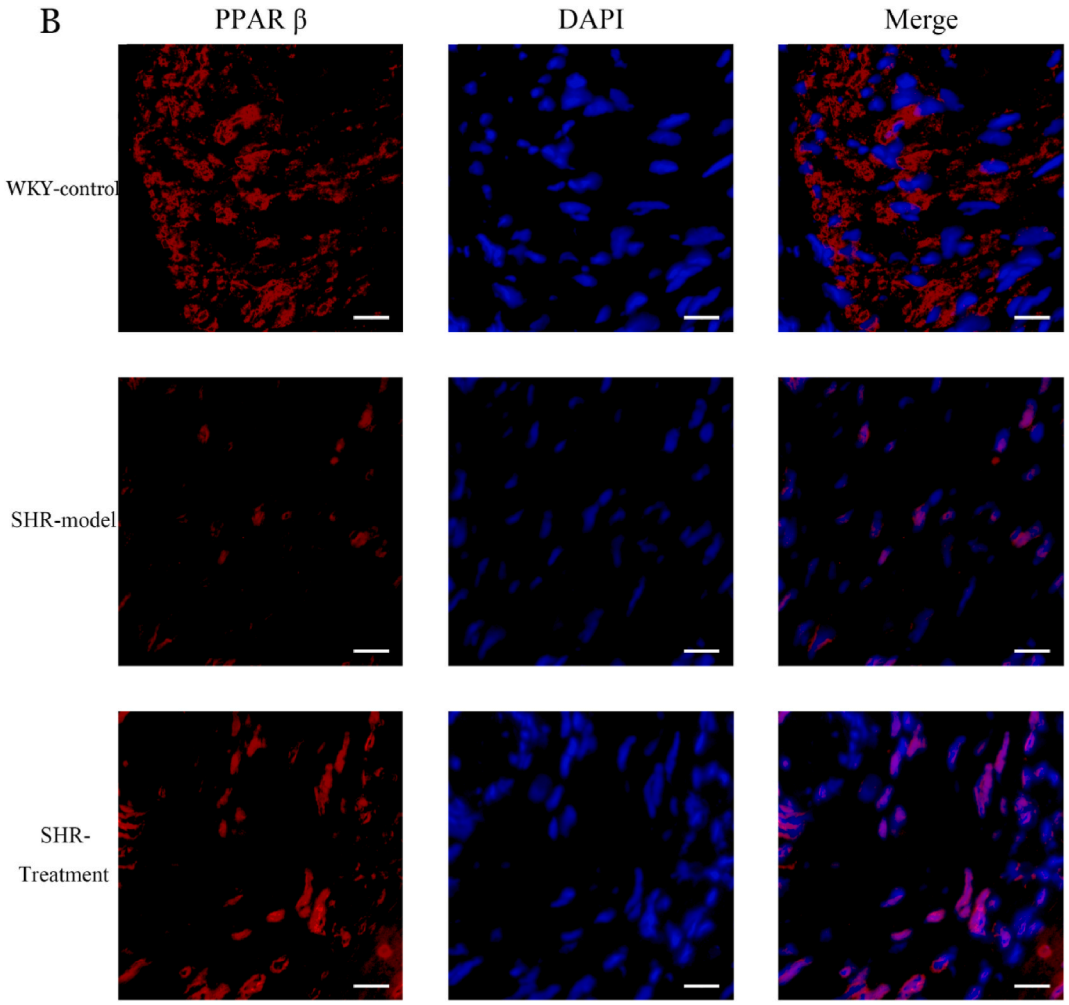

Fig. 7. (*continued*).

4. Discussion

SHRs are inbred genetic models of experimental hypertension. Their blood pressure rapidly increases to >180 mmHg between 6th and 12th week after birth, reaching a maximum value of 240 mmHg in the 24th week, accompanied by heart, brain, and kidney damage. Given that the progression of hypertension in SHRs is similar to that of human primary hypertension in many aspects [16], and that many potential antihypertensive agents have been identified using SHRs, this animal model was selected for the present study.

Blood pressure measurements showed that following administration of the synbiotic preparation, the SBP of SHRs in the treatment group decreased significantly in the 6th week compared with that of SHRs in the model group. After withdrawal of the synbiotic preparation, the SBP of the SHRs in the treatment group rapidly recovered within 2 weeks to almost the same level as that in the model group. Following readministration of the synbiotic preparation, the SBP of SHRs in the treatment group improved. These data indicate that the synbiotic preparation may exert an antihypertensive effect in SHRs. However, the DBP of SHRs in the treatment group did not change significantly compared to that of SHRs in the model group. Moreover, plasma levels of AII, COR, and ALD were not significantly different between the treatment and model groups. SBP constitutes the highest arterial blood pressure in the cardiac cycle and occurs immediately after systole of the left ventricle of the heart, representing the capability of cardiac output that is dependent on myocardial systole and aortic distention; whereas DBP constitutes the lowest arterial blood pressure of the cardiac cycle and occurs during diastole of the heart, reflecting the extent of peripheral vascular resistance [17]. AII strongly contracts the blood vessels and increases peripheral vascular resistance, leading to elevated blood pressure. AII also stimulates the adrenal cortical zona cells to synthesize and release ALD, which increases blood volume and blood pressure [18]. COR, a glucocorticoid, is secreted by the adrenal cortex band cells and regulates glucose metabolism and electrolyte distribution. Overproduction of COR leads to hypertension [19]. Therefore, SBP and DBP are regulated by the RAAS. However, notably, our data indicate that the antihypertensive mechanism of the synbiotic preparation does not involve the RAAS.

Because gut microbiota-mediated antihypertensive effects may involve attenuation of systemic dysfunction in the host via

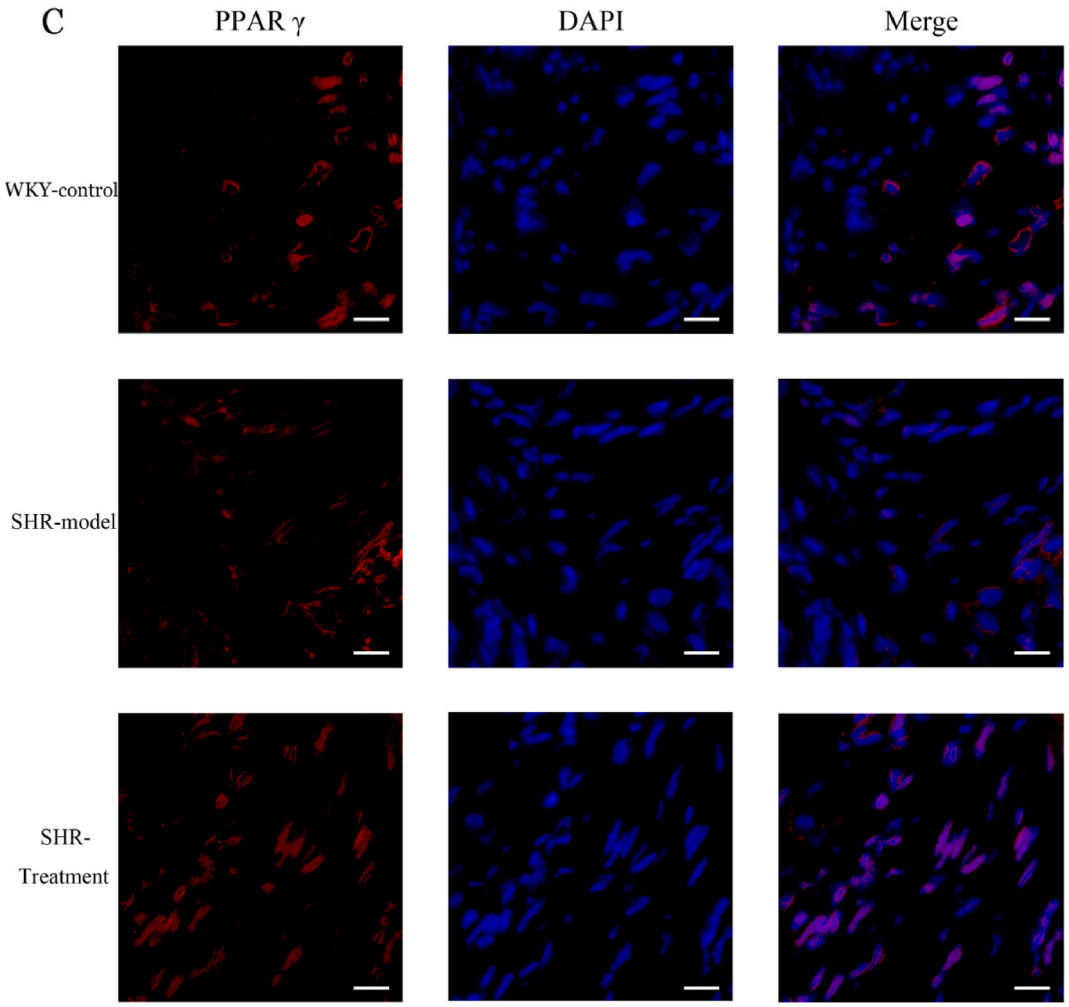

Fig. 7. (*continued*).

interactions of the local microbiota in the gastrointestinal tract, we examined the colonization of the gastrointestinal tract by *L. acidophilus* and *B. lactis* from the synbiotic preparation and the underlying antihypertensive mechanism using molecular biological techniques, proteomics, metabolomics, and immunohistochemistry.

Following 7 weeks of continuous administration of SHRs with the synbiotic preparation, both *L. acidophilus* and *B. lactis* predominately colonized the ileum and colon, and the quantities of both *L. acidophilus* and *B. lactis* were significantly higher in the ileum and colon than that in the jejunum. The entire intestinal mucosal surface is covered with a thick layer of mucus gel (>100 μm) secreted by goblet cells that protects the epithelial lining from luminal sheer forces, adhesion, and invasion by microorganisms, dietary toxins, and other antigens present in the intestinal lumen. The intestinal mucus consists of two layers with similar protein composition. The inner layer is firmly attached to the epithelium and functions as a barrier to prevent bacterial invasion, whereas the outer layer consists of a loose matrix that is generally colonized by bacteria. Several studies have demonstrated that the thickness of the mucus layer varies along the intestine and is thickest in the colon and thinnest in the jejunum. The rate of mucus secretion and extent of mucus accumulation provide a suitable environment for endogenous microflora [20,21] and contribute to *L. acidophilus* and *B. lactis* colonization of the ileum and colon. Moreover, a symbiotic relationship exists between *L. acidophilus* and *B. lactis*; namely, vitamin B and folic acid released by *B. lactis* promotes *L. acidophilus* proliferation, which in turn produces nutrients for *B. lactis*, all of which are conducive to the co-colonization of both microorganisms in the ileum and colon. In addition, xylooligosaccharides in the synbiotic preparation facilitate the co-colonization of *B. lactis* and *L. acidophilus* in the gastrointestinal tract [22].

Proteomics is an powerful tool to study hypertensive conditions and related mechanisms, and has been widely used to study hypertension since 2001 [23,24]. In the present study, KEGG pathway enrichment analysis of the 71 differentially expressed proteins in the ileum indicated that the mechanism underlying hypertension in SHRs may involve the PPAR signaling pathway. Six proteins related to this pathway were upregulated or downregulated in the model group (acyl-CoA oxidase, apolipoprotein A1, and carnitine palmitoyltransferase 2 expression were upregulated, whereas CD36, acyl-CoA synthetase long chain family member, and RXRβ expression were downregulated). Moreover, these proteins were modulated by the synbiotic preparation. These results further suggest

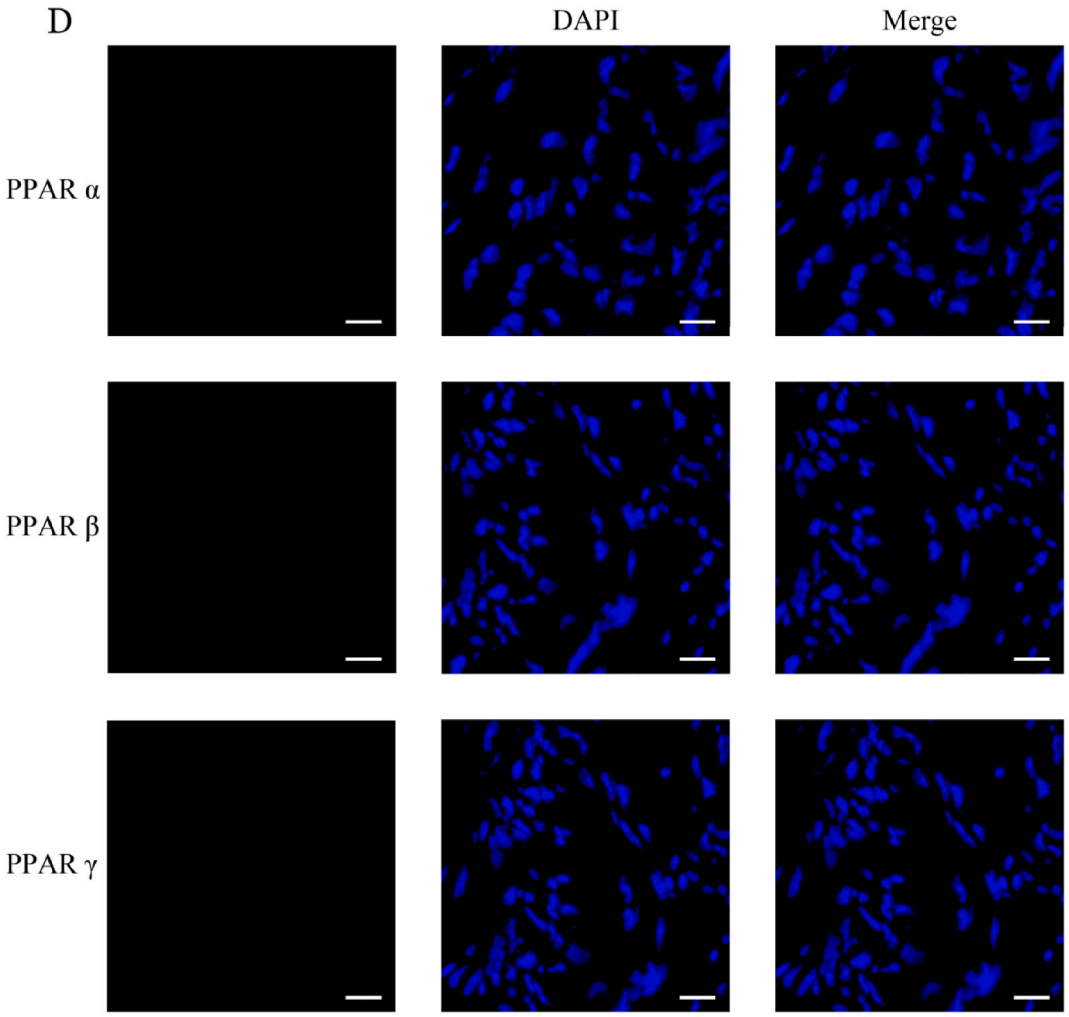

Fig. 7. (*continued*).

that the synbiotic preparation may regulate the PPAR signaling pathway to improve the blood pressure of SHRs by facilitating the interaction of the two colonizing microorganisms with the cells of the small intestine. Based on the above results, it is conceivable that in the lumen of the small intestine of a healthy host, fatty acids and their metabolites, the major bacterial fermentation products of carbohydrates, lipids, and proteins, are transported across the cell membrane by binding to fatty acid translocase (FAT/CD36) on the membrane, and are then transported into the nucleus by binding to fatty acid-binding protein (FABP) in the cytoplasm. After entering the nucleus, the complex consisting of FABP and the ligand bound to the PPAR receptor forms a heterodimer with RXR, which activates the transcriptional machinery through the recruitment of coregulators. The transcriptional machinery regulates gene expression by binding to specific DNA sequence elements, termed PPAR response elements, which activate the biochemical cascade reactions of PPARs. However, hypertension, a chronic disease, may cause dysbiosis of the endogenous microflora community in the gastrointestinal tract of the host and lead to the loss of probiotics. This disruption may decrease the amount and absorption of fatty acids and their metabolites produced by probiotics by the cells of the small intestine, which may in turn attenuate the PPAR signaling pathway to exacerbate hypertension. Following administration of the synbiotic preparation, *L. acidophilus* and *B. lactis* colonize the gastrointestinal tract of SHRs and restore the balance of endogenous microflora, which leads to restoration of the PPAR signaling pathway to improve hypertension. Notably, among the six PPAR pathway-related proteins identified in the present study, RXRβ, a key nodal protein in this pathway, was significantly reregulated following administration of the synbiotic preparation. The reason for the specific and significant reregulation of RXRβ by the symbiotic preparation compared to the other PPAR pathway-related proteins may be attributed to the inadequate intervention (in terms of the duration and dosage of the preparation) or inadequate numbers of samples analyzed, all of which merit further exploration.

PPARs belong to the nuclear hormone receptor superfamily of transcription factors, and comprise of three distinct subtypes PPAR α, β/δ, and γ, all of which are expressed in the small intestine [25]. We sought to determine which PPAR subtypes played a role in improving blood pressure. The results of immunohistochemistry revealed that the expression of PPARβ and γ was significantly

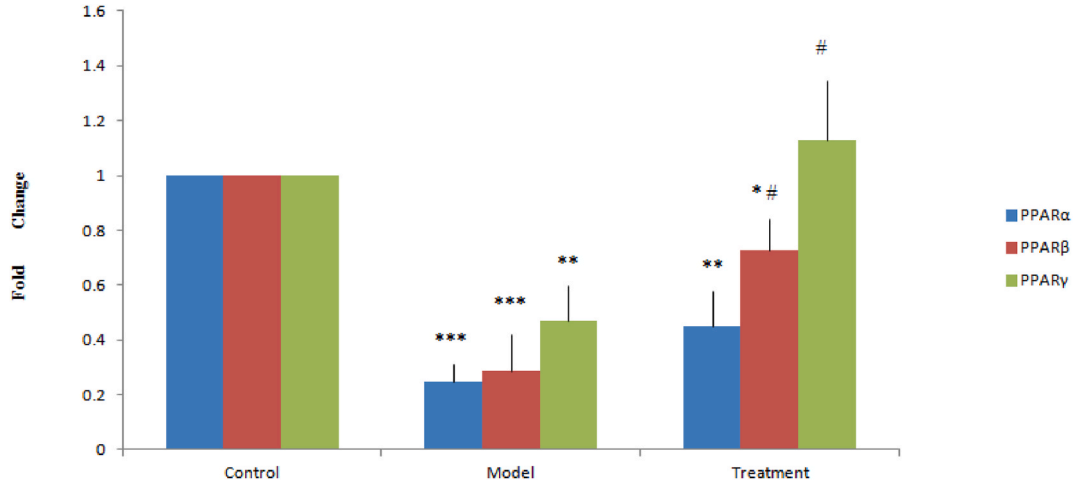

Fig. 8. The expressions of PPARα, β and γ in the ileum segments of the control, model and treatment groups were determined by the method of qPCR. All data were presented as the mean ± standard error of the mean. Asterisks indicated statistical significance between the SHR-model or the SHR-treatment group and the WKY-control group, *p < 0.05, **p < 0.01, ***p < 0.001. Symbol indicated statistical significance between the SHR-model and the SHR-treatment groups, #p < 0.05.

upregulated in the ileum of the treatment group compared with that of the model group, which further confirmed the proteomics results. Consistent with these results, administration of the PPARβ and γ antagonists GSK3787 and GW9662, significantly increased SBP that was lowered by the synbiotic preparation in the SHR treatment group. Several lines of evidence have shown that activation of PPARβ and γ improves eNOS-mediated vasodilatation by increasing antioxidant activity and inhibits the inflammatory response in the vascular wall by repressing NF-κB signaling, which, in turn, restores vascular structure and function to reduce blood pressure [26–28]. Activation of PPARβ was previously shown to cause a progressive reduction in SBP; however, not in DBP, in SHRs [28], which is consistent with the blood pressure data in the present study. Additionally, the metabolomic analysis indicated that the levels of lysoPE and PCs in the ileum were significantly higher in the treatment group than that in the model group. Several studies have reported that lysoPE and PCs released from intestinal bacterial fermentation and their metabolites, such as free fatty acids, specifically activate the PPAR pathway and induce PPAR expression [29–33]. Therefore, the synbiotic preparation may improve the blood pressure of SHRs by altering the composition of their intestinal microbiota, regulating PPAR signaling pathway, and activating the PPARβ and γ cascade in the ileum.

Although the synbiotic preparation contributed to the localization of *L. acidophilus* and *B. lactis* both in the ileum and colon of SHRs in the treatment group, the gut microbiota inhabiting the colon segment only ferments carbohydrates and proteins that escape absorption in the small intestine during digestion. The small intestine serves as the primary digestive and absorptive organ for a wide range of metabolites, such as short-chain fatty acids produced from the interaction of the microbiota with dietary components. These metabolites are effectively absorbed in the small intestine, and activate relevant biochemical cascade reactions, leading to changes in the physiology and pathology of the host. Given that the colon has a lower absorption efficacy than the ileum, it is unlikely to be the most important part of the gastrointestinal tract contributing to the synbiotic preparation-mediated improvement of the blood pressure of SHRs. However, this warrants further investigation.

5. Conclusions

In conclusion, the novel synbiotic preparation improves blood pressure by altering the composition of the intestinal microbiota, regulating PPAR signaling pathway, and activating the PPARβ and γ cascade reactions in the ileum.

Funding

The work was supported by grants from project of Natural Science Foundation of Liaoning Province (20170540927) and Shenyang Science and Technology Plan Project (22-321-33-33).

Data availability

Data will be made available on request.

CRediT authorship contribution statement

Ying Huang: Writing – review & editing, Validation, Conceptualization. **Fang Wang:** Conceptualization. **Wei Gong:** Writing –

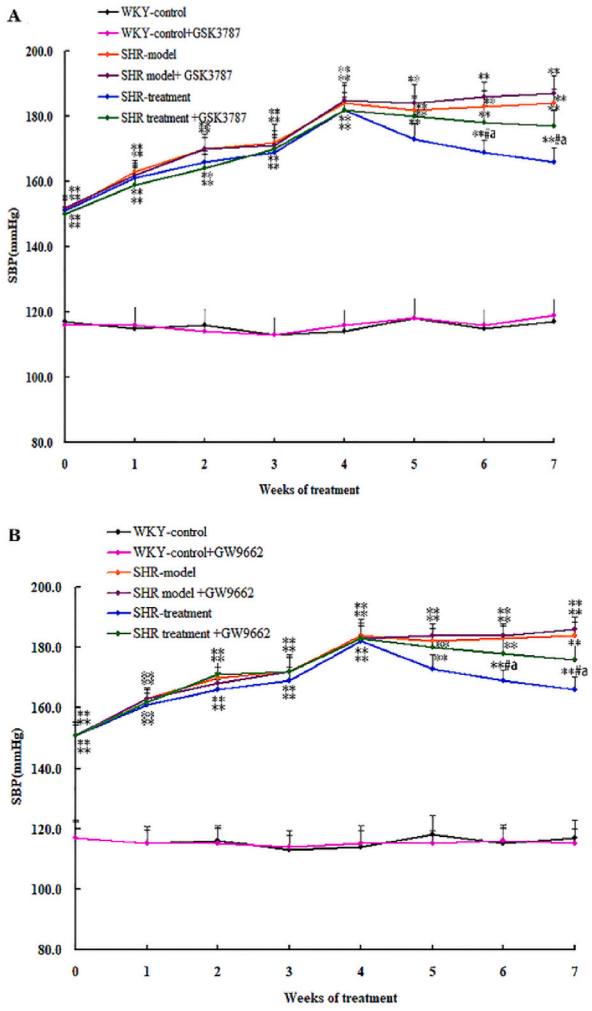

Fig. 9. (A) The effects of GSK3787 and synbiotics on SBP in the SHRs. In the first 4 weeks, there were no difference in SBP between SHR-model and SHR-treatment group, both of which showed the significant difference in comparison with WKY group. From Week 4 to Week 7, there were obviously difference in SBP between SHR-model and SHR-treatment group. However, after administered with GSK3787, the level of SBP of SHR-treatment group rebounded, which showed the significant difference, compared with that of SHR-treatment group without GSK3787. GSK3787 had no effects on the SHR-model and WKY group. The dots were presented as the mean ± standard error of the mean. Asterisks indicated statistical significance between the SHR-model or the SHR-treatment group and the WKY-control group on the same week, $^{**}p < 0.01$. Symbol indicated statistical significance between the SHR-model and the SHR-treatment groups on the same week, $\#p < 0.05$. Letter indicated statistical significance between the SHR-treatment without and with GSK3787, a $p < 0.05$.
(B) The effects of GW9662 and synbiotics on SBP in the SHRs. In the first 4 weeks, there were no difference in SBP between SHR-model and SHR-treatment group, both of which showed the significant difference in comparison with WKY group. From Week 4 to Week 7, there were obviously difference in SBP between SHR-model and SHR-treatment group. However, after administered with GW9662, the level of SBP of SHR-treatment group rebounded, which showed the significant difference, compared with that of SHR-treatment group without GW9662. GW9662 had no effects on the SHR-model and WKY group. The dots were presented as the mean ± standard error of the mean. Asterisks indicated statistical significance between the SHR-model or the SHR-treatment group and the WKY-control group on the same week, $^{**}p < 0.01$. Symbol indicated statistical significance between the SHR-model and the SHR-treatment groups on the same week, $\#p < 0.05$. Letter indicated statistical significance between the SHR-treatment without and with GW9662, a $p < 0.05$.

original draft, Formal analysis. **Yufeng Chen:** Writing – review & editing.

Declaration of competing interest

It is the first time to submit the research article to **Heliyon**. This manuscript is based on the original research results and has never been published elsewhere. We warrant that all of the authors have contributed substantially to the manuscript and approved the final submission. If accepted, it will not be published elsewhere in the same form, in English or in any other language.

Acknowledgements

We thank Dr. Miao Liu for the suggestion of experiments.

References

[1] P. Kramer, P. Bressan, Humans as superorganisms: how microbes, viruses, imprinted genes, and other selfish entities shape our behavior, Perspect. Psychol. Sci. 10 (2015) 464–481.
[2] T. Yatsunenko, F.E. Rey, M.J. Manary, I. Trehan, M.G. Dominguez-Bello, M. Contreras, M. Magris, G. Hidalgo, R.N. Baldassano, A.P. Anokhin, et al., Human gut microbiome viewed across age and geography, Nature 486 (2012) 222–227.
[3] S. Tims, C. Derom, D.M. Jonkers, R. Vlietinck, W.H. Saris, M. Kleerebezem, W.M. de Vos, E.G. Zoetendal, Microbiota conservation and BMI signatures in adult monozygotic twins, ISME J. 7 (2013) 707–717.
[4] P.J. Turnbaugh, M. Hamady, T. Yatsunenko, B.L. Cantarel, A. Duncan, R.E. Ley, M.L. Sogin, W.J. Jones, B.A. Roe, J.P. Affourtit, et al., A core gut microbiome in obese and lean twins, Nature 457 (2009) 480–484.
[5] G.Z. Erwin, D.L.A. Antoon, M.A.V. Wilma, J.G.M.V. Arjan, M.V. Willem, The host genotype affects the bacterial community in the human gastronintestinal tract, Microb. Ecol. Health Dis. 13 (2001) 129–134.
[6] T. Nwankwo, S.S. Yoon, V. Burt, Q. Gu, Hypertension Among Adults in the United States: National Health and Nutrition Examination Survey, 2011-2012, vol. 133, NCHS Data Brief, 2013, pp. 1–8.
[7] J. Yang, Y.N. Chen, Z.X. Xu, Y. Mou, L.R. Zheng, Alteration of RhoA prenylation ameliorates cardiac and vascular remodeling in spontaneously hypertensive rats, Cell. Physiol. Biochem. 39 (2016) 229–241.
[8] R.W. Schmid, J. Lotz, R. Schweigert, K. Lackner, G. Aimo, J. Friese, T. Rosiere, D. Dickson, D. Kenney, G.T. Maine, Multi-site analytical evaluation of a chemiluminescent magnetic microparticle immunoassay (CMIA) for sirolimus on the Abbott ARCHITECT analyzer, Clin. Biochem. 42 (2009) 1543–1548.
[9] N.J. Puhl, R.R. Uwiera, L.J. Yanke, L.B. Selinger, G.D. Inglis, Antibiotics conspicuously affect community profiles and richness, but not the density of bacterial cells associated with mucosa in the large and small intestines of mice, Anaerobe 18 (2012) 67–75.
[10] M. Haarman, J. Knol, Quantitative real-time PCR analysis of fecal Lactobacillus species in infants receiving a prebiotic infant formula, Appl. Environ. Microbiol. 72 (2006) 2359–2365.
[11] T. Maniatis, F.E. Fritsch, J. Sambrook, Molecular Cloning: a Laboratory Manual, third ed., Cold Spring Harbor Laboratory Press, revised, 1982.
[12] R.R. Shirima, D.G. Maeda, E. Kanju, G. Ceasar, F.I. Tibazarwa, J.P. Legg, Absolute quantification of cassava brown streak virus mRNA by real-time qPCR, J Virol Methods 245 (2017) 5–13.
[13] S. Wu, Y. Gao, X. Dong, G. Tan, W. Li, Z. Lou, Y. Chai, Serum metabonomics coupled with Ingenuity Pathway Analysis characterizes metabolic perturbations in response to hypothyroidism induced by propylthiouracil in rats, J. Pharm. Biomed. Anal. 72 (2013) 109–114.
[14] H. Zhao, H. Du, M. Liu, S. Gao, N. Li, Y. Chao, R. Li, W. Chen, Z. Lou, X. Dong, Integrative proteomics-metabolomics strategy for pathological mechanism of vascular depression mouse model, J. Proteome Res. 17 (2018) 656–669.
[15] Y. Li, J. Tao, J. Zhang, X. Tian, S. Liu, M. Sun, X. Zhang, C. Yan, Y. Han, Cellular repressor E1A-stimulated genes controls phenotypic switching of adventitial fibroblasts by blocking p38MAPK activation, Atherosclerosis 225 (2012) 304–314.
[16] M. Pravenec, T.W. Kurtz, Recent advances in genetics of the spontaneously hypertensive rat, Curr. Hypertens. Rep. 12 (2010) 5–9.
[17] S. Pede, M. Lombardo, Definizione del rischio cardiovascolare. Pressione arteriosa sistolica, diastolica o differenziale? [Cardiovascular risk stratification. Systolic, diastolic or pulse pressure?], Ital. Heart J. Suppl. 2 (2001) 356–358.
[18] L. Te Riet, J.H. van Esch, A.J. Roks, A.H. van den Meiracker, A.H. Danser, Hypertension: renin-angiotensin-aldosterone system alterations, Circ. Res. 116 (2015) 960–975.
[19] L.C. Martins, F.L. Conceição, E.S. Muxfeldt, G.F. Salles, Prevalence and associated factors of subclinical hypercortisolism in patients with resistant hypertension, J. Hypertens. 30 (2012) 967–973.
[20] M.E. Johansson, J.M. Larsson, G.C. Hansson, The two mucus layers of colon are organized by the MUC2 mucin, whereas the outer layer is a legislator of host-microbial interactions, Proc Natl Acad Sci U S A. 108 (Suppl 1) (2011) 4659–4665. Suppl 1.
[21] C. Atuma, V. Strugala, A. Allen, L. Holm, The adherent gastrointestinal mucus gel layer: thickness and physical state in vivo, Am. J. Physiol. Gastrointest. Liver Physiol. 280 (2001) G922–G929.
[22] S.H. Lin, L.M. Chou, Y.W. Chien, J.S. Chang, C.I. Lin, Prebiotic effects of xylooligosaccharides on the improvement of microbiota balance in human subjects, Gastroenterol Res Pract 2016 (2016) 5789232.
[23] C. Delles, U. Neisius, D.M. Carty, Proteomics in hypertension and other cardiovascular diseases, Ann. Med. 44 (Suppl 1) (2012) S55–S64.
[24] G. Currie, C. Delles, The future of "omics" in hypertension, Can. J. Cardiol. 33 (2017) 601–610.
[25] W. Wahli, L. Michalik, PPARs at the crossroads of lipid signaling and inflammation, Trends Endocrinol Metab 23 (2012) 351–363.
[26] Q.N. Diep, M. El Mabrouk, J.S. Cohn, D. Endemann, F. Amiri, A. Virdis, M.F. Neves, E.L. Schiffrin, Structure, endothelial function, cell growth, and inflammation in blood vessels of angiotensin II-infused rats: role of peroxisome proliferator-activated receptor-gamma, Circulation 105 (2002) 2296–2302.
[27] J.M. Kleinhenz, D.J. Kleinhenz, S. You, J.D. Ritzenthaler, J.M. Hansen, D.R. Archer, R.L. Sutliff, C.M. Hart, Disruption of endothelial peroxisome proliferator-activated receptor-gamma reduces vascular nitric oxide production, Am. J. Physiol. Heart Circ. Physiol. 297 (2009) H1647–H1654.
[28] M.J. Zarzuelo, R. Jiménez, P. Galindo, M. Sánchez, A. Nieto, M. Romero, A.M. Quintela, R. López-Sepúlveda, M. Gómez-Guzmán, E. Bailón, et al., Antihypertensive effects of peroxisome proliferator-activated receptor-β activation in spontaneously hypertensive rats, Hypertension 58 (2011) 733–743.
[29] Q. Zhao, X.M. Li, H.N. Liu, F.J. Gonzalez, F. Li, Metabolic map of osthole and its effect on lipids, Xenobiotica 48 (2018) 285–299.
[30] F.J. Schopfer, Y. Lin, P.R. Baker, T. Cui, M. Garcia-Barrio, J. Zhang, K. Chen, Y.E. Chen, B.A. Freeman, Nitrolinoleic acid: an endogenous peroxisome proliferator-activated receptor gamma ligand, Proc Natl Acad Sci U S A 102 (2005) 2340–2345.
[31] J.M. Del Bas, A. Caimari, M.I. Rodriguez-Naranjo, C.E. Childs, C. Paras Chavez, A.L. West, E.A. Miles, L. Arola, P.C. Calder, Impairment of lysophospholipid metabolism in obesity: altered plasma profile and desensitization to the modulatory properties of n-3 polyunsaturated fatty acids in a randomized controlled trial, Am. J. Clin. Nutr. 104 (2016) 266–279.
[32] A. Pathil, G. Liebisch, J.G. Okun, W. Chamulitrat, G. Schmitz, W. Stremmel, Ursodeoxycholyl Lysophosphatidylethanolamide modifies aberrant lipid profiles in NAFLD, Eur. J. Clin. Invest. 45 (2015) 925–931.
[33] N.Y. Kim, T.H. Kim, E. Lee, N. Patra, J. Lee, M.O. Shin, S.J. Kwack, K.L. Park, S.Y. Han, T.S. Kang, et al., Functional role of phospholipase D (PLD) in di(2-ethylhexyl) phthalate-induced hepatotoxicity in Sprague-Dawley rats, J. Toxicol. Environ. Health 73 (2010) 1560–1569.